Contrib Mineral Petrol
DOI 10.1007/s00410-007-0251-3

ORIGINAL PAPER

Subduction cycling of volatiles and trace elements through the Central American volcanic arc: evidence from melt inclusions

Seth J. Sadofsky · Maxim Portnyagin · Kaj Hoernle · Paul van den Bogaard

Received: 8 December 2006 / Accepted: 3 September 2007

Abstract Compositions of melt inclusions in olivine (Fo_{90-64}) from 11 localities in Guatemala, Nicaragua and Cost Rica along the Central American Volcanic Arc are used to constrain combined systematics of major and trace elements and volatile components (H_2O, S, Cl, F) in parental melts and to estimate volcanic fluxes of volatile elements. The melt inclusions cover the entire range of compositions reported for whole rocks from Central America. They point to large heterogeneity of magma sources on local and regional scales, related to variable contributions of diverse crustal (from the subducting and overriding plates) and mantle (from the wedge and incoming plate) components involved in magma genesis. Water in parental melts correlates inversely with Ti, Y and Na and positively with Ba/La and B/La (with the exception of Irazú Volcano), which indicates mantle melting fluxed by Ba-, B- and H_2O-rich, possibly, serpentinite-derived fluid beneath most parts of the arc. Different components with melt-like characteristics (high LREE, La/Nb and probably also Cl, S and F and low Ba/La) control the geochemical peculiarities of Guatemalan and Costa Rican magmas. The composition of parental magmas together with published data on volcanic volumes and total SO_2 flux from satellite measurements are used to constrain fluxes of volatile components and to estimate total magmatic flux in Central America. We found that volcanic flux accounts for only 13% of total magmatic and volatile fluxes. The remaining 87% of magmas remained in the lithosphere to form cumulates (~39%) and intrusives (~48%). The intrusive fraction of magmatic flux may be significantly larger beneath Nicaragua compared to Costa Rica. Interestingly, total fluxes of magmas and volatiles in Central America are quite similar to the global average estimates.

Communicated by J. Hoefs.

Electronic supplementary material The online version of this article (doi:10.1007/s00410-007-0251-3) contains supplementary material, which is available to authorized users.

S. J. Sadofsky · K. Hoernle · P. van den Bogaard
SFB 574, University of Kiel, Wischhofstr. 1-3,
Kiel 24148, Germany

M. Portnyagin (✉) · K. Hoernle · P. van den Bogaard
Leibniz Institute for Marine Sciences (IFM-GEOMAR),
Wischhofstr. 1-3, Kiel 24148, Germany
e-mail: mportnyagin@ifm-geomar.de

M. Portnyagin
Vernadsky Institute, Kosigin st. 19, 119991 Moscow, Russia

Introduction

Subduction zones provide the return flux of water and other volatiles from the surface of the earth to the mantle, making our understanding of global volatile cycling heavily reliant on understanding subduction zone magmatism. Composition of the crustal input, dip of the subducting slab and volcanic output vary along the Central American subduction zone (Fig. 1) (Carr et al. 1990, 2003; Patino et al. 2000; Protti et al. 1995; Rüpke et al. 2002). These differences may have a major influence on elemental, and especially volatile, cycling through the subduction system. In particular, it was proposed that the steeply dipping oceanic plate subducting beneath Nicaragua was highly hydrated, thus delivering larger amounts of water and other volatiles into the mantle wedge beneath this segment of the Central American Volcanic Arc (CAVA), explaining the distinct geochemistry of the volcanic output

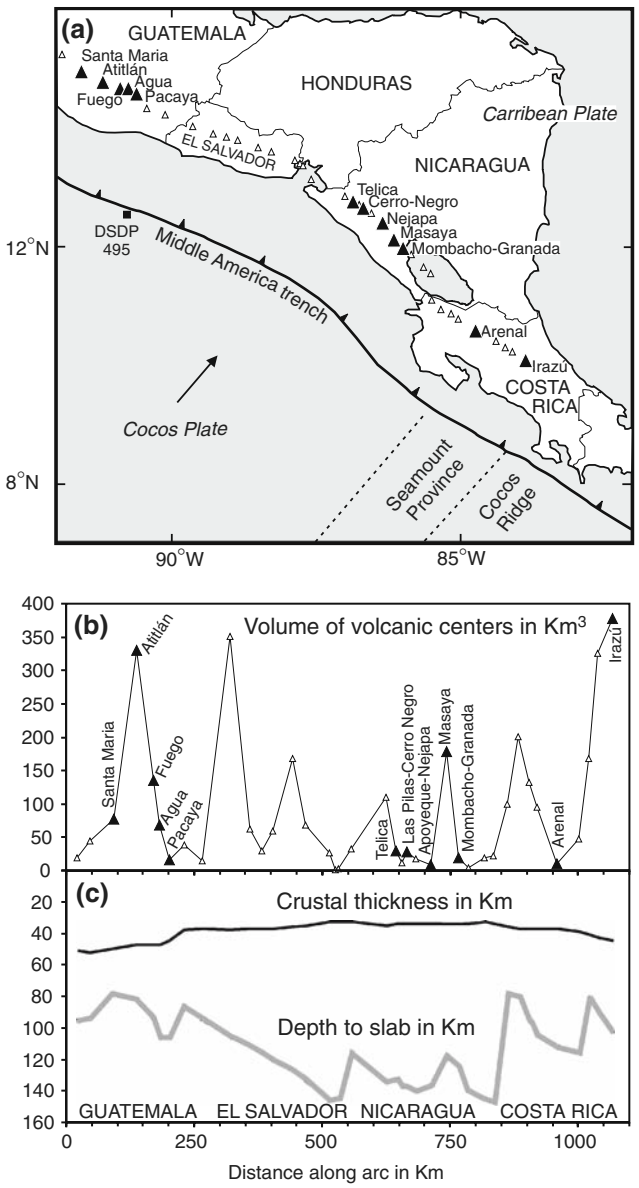

Fig. 1 Geologic framework of the Central American arc magmatism. **a** Schematic map showing the Central American volcanic arc, formed in response to the subduction of the Cocos Plate beneath the Caribbean Plate. The Cocos Ridge and Seamount Province belong to the Galapagos hotspot track subducting beneath southern Costa Rica. *Triangles* illustrate locations of frontal volcanoes with localities of samples selected for this melt inclusion study denoted by *filled triangles*. *Thin lines* are country boundaries. **b** Volumes of volcanic centers along the volcanic front in Central America (Carr et al. 2003). **c** Variations in crustal thickness (Carr et al. 2003) and depths to subducting plate (Syracuse and Abers 2006) along the volcanic front in the Central America. Here and in the following plots the distance was measured from the Mexican-Guatemalan border

(Abers et al. 2003; Ranero et al. 2003; Rüpke et al. 2002). The quantity of volatiles in the Central American magmas, and the magmatic volatile fluxes and their correlations with major and trace element geochemistry and magmatic productivity are however poorly understood but absolutely necessary for understanding the magma generation processes in the arc system.

Studies of melt inclusions in early-crystallizing phenocryst phases provide direct insights into pre-eruptive water (and other volatile) contents in magmas (Harris and Anderson 1984; Portnyagin et al. 2007; Sobolev and Chaussidon 1996; Wallace 2005). Previous studies of the volatile content in mafic magmas from Central America found high H_2O concentrations in the volcanic front (up to 6% for Cerro Negro in Nicaragua) (Benjamin et al. 2007; Roggensack et al. 1997, 2001b; Sisson and Layne 1993; Wade et al. 2006; Walker et al. 2003) and substantially lower contents in back-arc cinder cones in Guatemala (Walker et al. 2003). Although the amount of available data has continuously increased over the past decade, there has been no attempt to present a regional picture of volatile abundances in the Central America magmas in conjunction with major and trace element systematics.

Here, we present new data on the composition of olivine-hosted melt inclusions from all major types of rocks in Guatemala, Nicaragua and Costa Rica to address several questions which are vital to our understanding of the Central American Subduction Zone: (1) What are the volatile (H_2O, S, Cl, F) concentrations of primitive magmas throughout Central America? (2) To what degree do trace element contents and their ratios correlate with the amount of H_2O in magmas? (3) What are the volcanic volatile fluxes for the different arc segments, and how do they correlate with subduction input?

Geologic setting

The geologic framework of volcanism in Central America has been extensively discussed in the literature (e.g. Aubouin et al. 1982; Carr et al. 1990, 2003; Leeman et al. 1994; Protti et al. 1995). In brief, volcanism in Central America results from the subduction of the Cocos Plate beneath the Caribbean Plate (Fig. 1a). From Guatemala to northern Costa Rica, ~25 Ma old crust formed at the East Pacific Rise subducts at a rate of about 80 mm/year and at an angle varying from 55° in Guatemala and El Salvador to 60–65° in Nicaragua and northern Costa Rica (Protti et al. 1995; Syracuse and Abers 2006) (Fig. 1). The sediment input is well-defined from Deep Sea Drilling Project (DSDP) Site 495 (Fig. 1). It can be divided into two layers: an ~200-m thick layer of hemipelagic clay overlies an ~250-m-thick layer of carbonate oozes (Aubouin et al. 1982; Plank and Langmuir 1998). It has been proposed that the mantle section of the oceanic plate subducting beneath Nicaragua contains a substantial amount of serpentinites (Abers et al. 2003; Ranero et al. 2003; Rüpke et al. 2002). Beneath central Costa Rica, ~15–20 Ma oceanic crust, formed at

the Galápagos Spreading Center and overprinted by the Galápagos Hotspot (Hoernle et al. 2000; Werner et al. 1999, 2003), subducts at a relatively shallow angle of ~50°. Crustal thickness decreases from 50 to <35 km from Guatemala to Nicaragua and increases up to ~45 km beneath Costa Rica, with the transition from continental in Guatemala to oceanic character of the basement beneath the southern part of the volcanic belt (Carr et al. 1990). Combined variations in subduction dip, crustal thickness and off-set of volcanic front from the trench result in large variations in the length of mantle columns beneath frontal volcanoes in Central America, which increases from ~40 km in Guatemala to 85–110 km in Nicaragua and sharply decreases to 45–75 km beneath Costa Rica (Fig. 1c).

Methods

Fresh samples of young (primarily historic) mafic tephra were collected from active volcanic centers in Guatemala, Nicaragua and Costa Rica. Hand-picked olivine phenocrysts (0.5–1 mm) were mounted in epoxy, polished and analyzed optically to locate melt inclusions. Inclusions selected for chemical analyses were glassy and usually contained homogeneous glass (± shrinkage bubble). A small number of inclusions from all regions contained sulfide globules and/or spinel crystals.

Major elements, Cl and S of glass inclusions and major element composition of olivine were analyzed by a CAMECA SX50 electron microprobe at IFM-GEOMAR. Major elements in olivine were analyzed with a 15-kilovolt (kV), 30-nanoampere (nA) beam 1.2 μm in diameter with a 20-s count time per element. Major elements in glass inclusions were analyzed with 15-kv, 10-nA beam, 5 μm in diameter with a 20-s count time per element. Chlorine and S were analyzed with 15-kV, 30-nA beam, 5 μm in diameter with a 60-s count time per element. Sulfur was measured at S^{6+} wavelength, and thus can be underestimated up to maximum 30 relative % due to possible presence of reduced S species in the glasses (Carroll and Rutherford 1988). Calibration was performed using pure oxides from CAMECA and natural reference materials (Jarosewich et al. 1980). San Carlos olivine (USNM 111312/444), basaltic glass VG-2 (USNM 111240/52) and scapolite (USNM R6600-1) were used as monitors during routine measurements. Values reported here are averages of at least three points per glass inclusion. Trace elements, fluorine and hydrogen concentrations were determined using a CAMECA ims4f ion microprobe at the Institute of Microelectronics and Informatics (Yaroslavl, Russia). Trace elements were determined with a primary beam of O^{2-} ions 20–30 μm in diameter at 14.5 kV and 15–20 nA current. Each analysis is based on five cycles of measurement with count times varying to provide appropriate counting statistics. Conversion of measured ion intensities to concentrations followed standard procedures (Portnyagin et al. 2002; Sobolev and Chaussidon 1996). Electron microprobe and ion microprobe data agree within estimated error (10% relative to concentration) as shown by comparison of Ti concentrations.

Any Fe–Mg disequilibrium between melt inclusions and host olivines is assumed to be due to post-entrapment crystallization of olivine, and is corrected by simulating incremental addition of equilibrium olivine to the melt inclusion composition until achieving equilibria with the host (Danyushevsky et al. 2002). The amount of olivine added was within 3–5 mol% in most cases. The following results and discussion refer to the compositions corrected for post-entrapment crystallization of olivine on the inclusion walls.

Results

Major elements

We present melt inclusion data of olivine phenocrysts from 11 sites in Guatemala, Nicaragua and Costa Rica. These include Santa Maria, Fuego, Agua and Atitlán Volcanoes in Guatemala; Cerro Negro and Masaya Volcanoes, a small tuff ring near Telica Volcano and cinder cones of the Nejapa and Granada lineaments in Nicaragua; and Irazú and Arenal Volcanoes in Costa Rica (Fig. 1). Major and trace element compositions of whole-rock samples selected for this melt inclusion study are given in the electronic supplement.

Melt-inclusion-bearing olivine phenocrysts in studied samples have forsterite content (100 Mg/(Mg + Fe), mol%) from 64 to 90 (Table 1; Fig. 2). The most magnesian olivines were found at Irazú (up to Fo_{90}) and Granada (up to Fo_{87}) samples. Typical olivine range in other samples is $Fo_{82–70}$, but as low as Fo_{64} at Atitlán. The olivine phenocryst compositions exhibit a general trend of decreasing maximum Fo from Costa Rica to Guatemala.

Studied melt inclusions are largely basaltic to basaltic andesitic in composition, similar to the most mafic whole-rock samples from Central America. Andesitic inclusions were found in evolved olivines ($Fo_{70–64}$) from Atitlán and Irazú Volcanoes. Major element compositions of melt inclusions (Table 1, Fig. 2) are generally similar to whole-rock compositions from the same areas and exhibit clear regional variations, which are particularly evident from comparison of a statistically significant number of inclusions from Guatemala and Nicaragua trapped in olivines with similar (moderately magnesian) compositions.

Table 1 Representative compositions of melt inclusions in olivine from the Central American volcanic arc

Volcano		Santa Maria	Fuego	Atitlán	Agua	Telica	Cerro Negro	Cerro Negro	Cerro Negro	Nejapa	Nejapa	Masaya	Granada	Granada	Granada	Arenal	Irazú	Irazú	Irazú	Irazú
Segment		GU	GU	GU	GU	NWN	NWN	NWN	NWN	SEN	SEN	SEN	SEN	SEN	SEN	CR	CR	CR	CR	CR
Rock sample		GU-19d	GU-3a	GU-25b	GU-11d	P2-16	P2-3a	P2-3a	P2-3a	P2-32d	P2-32d	P2-47	P2-58	P2-58	P2-58	CR-61C	P2-72	P2-72	P2-72	P2-72
Inclusion#		s1	1	s1	s7	9	1-10	1-35	2-46a	4a	6a	3a	27a	8	2-69	57	40a	40b	3-1	3-2
Melt inclusions																				
SiO_2 (wt%)	EMP	53.07	56.78	54.97	50.90	47.00	48.10	49.44	49.53	47.26	48.74	53.71	52.20	47.57	47.98	50.94	60.43	57.62	52.33	52.05
TiO_2 (wt%)	EMP	1.03	1.17	1.57	1.14	0.78	0.77	0.59	0.72	2.63	1.13	1.25	1.16	0.89	1.08	0.79	1.28	1.55	0.89	0.98
Al_2O_3 (wt%)	EMP	19.84	18.00	17.84	19.84	16.33	18.55	18.96	18.06	17.47	17.34	15.72	16.42	18.62	16.68	19.49	16.15	15.90	17.96	18.18
FeO* (wt%)	EMP	8.11	7.63	8.69	7.88	11.84	10.73	10.05	9.88	11.28	10.34	11.66	10.55	9.49	10.00	9.60	6.96	8.44	7.13	7.77
MnO (wt%)	EMP	0.10	0.15	0.12	0.07	0.25	0.18	0.24	0.17	0.22	0.19	0.23	0.16	0.17	0.18	0.16	0.12	0.11	0.15	0.17
MgO (wt%)	EMP	2.76	3.39	3.35	5.08	5.71	6.68	6.09	6.66	6.61	6.88	3.92	6.42	7.59	7.61	4.14	2.33	2.88	5.93	4.77
CaO (wt%)	EMP	10.48	7.30	8.38	10.20	14.06	12.74	12.31	12.65	11.19	12.89	8.80	9.84	13.18	14.08	11.65	3.63	4.39	11.65	11.75
Na_2O (wt%)	EMP	3.50	3.97	3.80	3.63	3.05	1.83	1.89	1.87	2.74	2.21	2.91	2.44	2.05	2.03	2.46	4.05	3.93	2.79	2.81
K_2O (wt%)	EMP	0.88	1.40	1.00	0.98	0.71	0.27	0.27	0.30	0.36	0.13	1.49	0.61	0.30	0.19	0.56	4.23	3.78	0.87	1.22
P_2O_5 (wt%)	EMP	0.23	0.21	0.28	0.28	0.28	0.13	0.17	0.17	0.26	0.15	0.31	0.21	0.15	0.17	0.21	0.82	1.39	0.30	0.29
Total (wt%)		100.00	100.00	100.00	100.00	100.00	100.00	100.00	100.00	100.00	100.00	100.00	100.00	100.00	100.00	100.00	100.00	100.00	100.00	100.00
Original total (wt%)		93.07	93.84	94.37	93.71	96.33	92.77	94.92	92.87	96.53	97.47	98.57	94.62	96.41	96.01	96.03	98.64	98.94	95.59	96.37
H_2O (wt%)	SIMS	3.5	3.8	3.3	3.4	3.0	5.2	4.8	4.9	1.9	2.1	1.7	5.0	3.7	2.6	1.6	1.0	1.0	5.2	3.0
S (ppm)	EMP	2278	1064	1388	1913	2408	1231	1031	1255	1482	1164	385	953	2071	1253	1625	282	345	1908	1461
Cl (ppm)	EMP	896	1017	1017	875	1628	960	689	749	298	264	1242	1111	889	329	1696	1455	2275	766	817
F (ppm)	SIMS	519	419	414	393	387	126	182	122	291	100	597	186	203	215	350	2143	3159	611	712
Li (ppm)	SIMS	7.9	12.9	10.7	6.5	4.5	3.6	3.7	3.6	3.7	3.3	11.0	5.9	4.1	4.7	5.7	18.9	20.2	5.0	14.2
Be (ppm)	SIMS	0.78	0.99	1.04	0.71	0.54	0.27	0.29	0.25	0.50	0.31	0.94	0.36	0.41	0.38	0.79	2.96	3.59	0.76	0.98
B (ppm)	SIMS	16.3	23.1	17.2	10.7	21.3	10.2	15.4	16.3	2.3	0.6	25.7	17.0	6.2	1.1	10.0	25.3	10.8	5.1	6.1
K (ppm)	SIMS	7332	11979	8603	7402	7172	2205	2248	2408	3817	1069	15274	5581	2632	1476	4482	33811	40620	7670	9393
Ti (ppm)	SIMS	5171	6107	8495	6215	4688	4229	3938	3897	17092	8169	8369	6928	5339	6986	4886	6538	9598	5286	5843
V (ppm)	SIMS	291	237	232	252	299	307	294	278	591	308	413	275	331	294	234	174	237	274	286
Cr (ppm)	SIMS	159	28	36	96	41	67	76	100	108	94	45	33	107	163	27	82	23	91	78
Sr (ppm)	SIMS	500	457	411	551	701	397	434	406	476	311	416	374	430	367	870	768	2652	792	826
Zr (ppm)	SIMS	76	102	101	95	46	18	21	20	98	47	113	38	31	51	51	317	431	60	71
Y (ppm)	SIMS	15	18	19	15	28	12	12	12	25	22	29	19	16	19	18	29	48	14	16
Nb (ppm)	SIMS	3.5	4.1	3.8	3.8	1.2	0.8	1.8	1.8	14.6	2.9	4.6	1.9	2.1	5.1	3.8	52	134	6.1	7.6
Ba (ppm)	SIMS	410	580	460	457	680	253	239	245	219	52	1140	493	206	79	529	1365	1895	467	531
La (ppm)	SIMS	9.0	11.1	10.3	10.9	7.8	2.1	2.6	2.6	6.7	2.8	14.4	5.4	3.4	4.0	14.4	75.9	144	17.7	22.1
Ce (ppm)	SIMS	19.5	24.1	23.8	23.1	16.4	4.9	5.8	5.6	17.8	7.8	27	9.9	8.1	11.0	27.5	158	318	36.2	45.4
Nd (ppm)	SIMS	11.1	13.0	15.1	13.9	14.3	4.4	4.6	4.4	14.0	7.1	19	7.8	6.6	8.8	15.9	70	125	17.7	22.1
Sm (ppm)	SIMS	3.2	3.4	4.0	3.7	4.4	1.5	1.6	1.6	4.0	2.7	4.9	2.3	2.0	2.9	3.4	12.2	21.1	3.9	4.5
Eu (ppm)	SIMS	2.1	1.2	1.1	1.0	1.9	0.7	0.5	0.7	1.6	1.1	2.5	1.4	0.8	1.1	1.3	2.8	3.7	1.2	1.5
Gd (ppm)	SIMS	1.5	3.3	3.5	2.3	5.1	2.3	2.1	1.6	3.9	3.5	4.8	2.9	2.6	3.1	4.1	9.9	15.1	3.3	4.1

Table 1 continued

Volcano		Santa Maria	Fuego	Atitlán	Agua	Telica	Cerro Negro	Cerro Negro	Cerro Negro	Nejapa	Nejapa	Masaya	Granada	Granada	Granada	Arenal	Irazú	Irazú	Irazú	Irazú
Segment		GU	GU	GU	GU	NWN	NWN	NWN	NWN	SEN	SEN	SEN	SEN	SEN	SEN	CR	CR	CR	CR	CR
Rock sample		GU-19d	GU-3a	GU-25b	GU-11d	P2-16	P2-3a	P2-3a	P2-3a	P2-32d	P2-32d	P2-47	P2-58	P2-58	P2-58	CR-61C	P2-72	P2-72	P2-72	P2-72
Inclusion#		s1	1	s1	s7	9	1-10	1-35	2-46a	4a	6a	3a	27a	8	2-69	57	40a	40b	3-1	3-2
Dy (ppm)	SIMS	2.5	2.9	3.3	2.8	5.1	2.0	2.2	2.0	4.1	3.5	4.9	2.9	2.7	3.1	3.4	6.7	10.5	2.5	3.1
Er (ppm)	SIMS	1.7	1.9	1.6	1.4	2.9	1.3	1.3	1.3	2.8	2.4	2.9	2.0	1.8	2.1	1.9	3.5	5.5	1.6	1.7
Yb (ppm)	SIMS	1.8	1.7	1.9	1.7	2.9	1.2	1.3	1.2	2.6	2.1	2.9	1.8	1.6	2.0	1.8	2.6	4.1	1.4	1.6
Hf (ppm)	SIMS	2.0	2.5	2.8	2.6	2.2	0.9	0.9	0.8	2.9	1.7	3.5	1.5	1.1	2.0	2.0	7.5	9.9	1.6	2.0
Th (ppm)	SIMS	0.70	1.5	1.1	0.7	0.5	0.10	0.12	0.14	0.32	0.09	1.7	0.39	0.14	0.16	1.06	14.9	10.2	1.6	2.6
U (ppm)	SIMS	0.22	0.76	0.5	0.3	0.5	0.13	0.09	0.11	0.20	0.03	1.6	0.39	0.15	0.09	0.43	6.3	3.6	0.63	0.80
Pb (ppm)	SIMS	3.0	5.0	4.5	4.4	3.5	0.80	1.14	1.23	1.01	0.32	6.6	2.0	1.2	0.8	3.0	8.5	15.6	1.8	3.1
Host olivine																				
Fo (mol%)		79.0	75.3	75.4	81.1	80.2	81.1	81.9	82.6	82.3	83.0	72.7	78.8	85.7	86.3	77.0	71.4	71.1	89.0	88.7
SiO_2 (wt%)	EMP	38.86	37.93	37.66	38.38	38.92	38.62	39.62	39.46	39.87	39.88	38.37	38.76	40.18	40.11	37.39	37.94	36.92	40.17	40.34
FeO (wt%)	EMP	19.62	22.52	22.39	17.57	18.67	17.76	17.06	16.52	16.81	16.21	24.71	19.65	13.77	13.20	21.22	25.69	25.97	10.71	11.01
MnO (wt%)	EMP	0.31	0.38	0.32	0.25	0.34	0.30	0.29	0.28	0.28	0.25	0.49	0.36	0.23	0.22	0.37	0.50	0.48	0.17	0.17
MgO (wt%)	EMP	41.29	38.61	38.50	42.27	42.34	42.65	43.37	43.92	43.71	44.26	36.88	40.98	46.44	46.66	39.95	35.99	35.83	48.55	48.65
CaO (wt%)	EMP	0.14	0.13	0.14	0.13	0.23	0.18	0.18	0.19	0.22	0.25	0.25	0.18	0.23	0.28	0.11	0.15	0.16	0.13	0.14
NiO (wt%)	EMP	0.06	0.07	0.08	0.11	0.07	0.09	0.10	0.11	0.15	0.19	0.08	0.06	0.19	0.21	0.11	0.11	0.11	0.39	0.35
Cr_2O_3 (wt%)	EMP	0.03	0.03	0.03	0.03	0.02	0.01	0.03	0.02	0.03	0.05	0.02	0.02	0.05	0.05	0.02	0.02	0.02	0.05	0.05
Total (wt%)		100.31	99.67	99.11	98.74	100.59	99.62	100.64	100.49	101.07	101.08	100.80	100.02	101.09	100.73	99.17	100.41	99.50	100.17	100.72

Notes. Major elements and S and Cl in melt inclusions and host olivines were determined by electron microprobe (EMP), trace elements by secondary ion mass spectrometry (SIMS). Complete data set of host rock compositions and studied melt inclusions is available on-line

Abbreviations for segments: *GU* Guatemala, *NWN* northwestern Nicaragua, *SEN* southeastern Nicaragua, *CR* Costa Rica

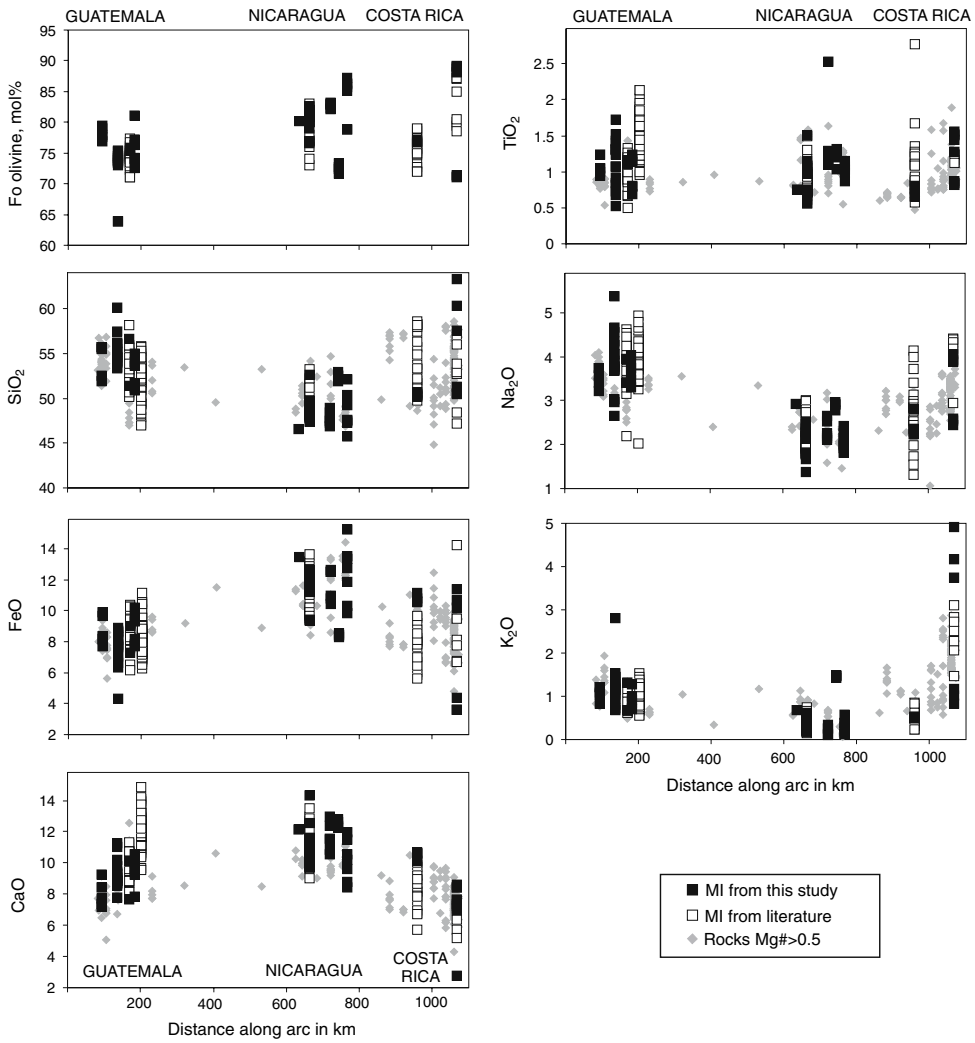

Fig. 2 Along arc variations of major element composition of melt inclusions and their host olivines. *Filled symbols* denote data from this study, *open symbols* data from olivine-hosted melt inclusions from the literature (Benjamin et al. 2007; Harris and Anderson 1984; Roggensack 2001a, b; Roggensack et al. 1997; Sisson and Layne 1993; Wade et al. 2006; Walker et al. 2003) and *small gray diamonds* compositions of primitive rocks with Mg# > 0.5 (Carr et al. 2003). Inclusions were recalculated to equilibrium with their host olivine using Petrolog 2.0 software (Danyushevsky et al. 2002), assuming oxygen fugacity at Ni–NiO buffer

Inclusions from Guatemala have distinctively higher SiO_2, Na_2O and lower FeO, MgO and CaO than inclusions from Nicaragua. Nicaragua inclusions generally have the lowest SiO_2 and Na_2O but highest FeO and CaO. Variations in TiO_2 concentrations along the volcanic front are not systematic. Inclusions in primitive olivines from Costa Rican volcanoes appear to have intermediate major element compositions between Nicaragua and Guatemala. Inclusions from Nicaragua and Arenal Volcano in Costa Rica have the lowest K_2O, with exception of evolved inclusions from Masaya, all below 1 wt%. Melts from Guatemala and Irazú volcano are more enriched, up to 3–5 wt% K_2O in evolved andesitic melts.

Trace elements

Trace element concentrations in the melt inclusions are highly variable on regional and local scales and generally fall within the range of reported whole-rock compositions (Table 1; Figs. 3, 4). In brief, melts from NW Nicaragua, particularly from Cerro Negro Volcano, have the lowest light rare earth element (LREE) and Th (<0.5 ppm) abundances and low La/Yb ratios (<3.5), but the highest ratios of fluid-mobile elements relative to REE and Th (Ba/La, Ba/Th, B/La, U/Th, Pb/Ce and Sr/Ce). Melts from Masaya Volcano in SE Nicaragua and Guatemalan volcanoes are systematically more enriched in LREE (La/Yb > 4), HFSE (Nb, Zr, Hf) and Th and have less pronounced slab-fluid signals (lower Ba/La, U/Th and B/La) compared to Cerro Negro Volcano. Primitive melts from Costa Rica, especially from Irazú Volcano, have distinct compositions from Guatemalan and Nicaraguan primitive melts and are distinctively enriched in nearly all highly incompatible trace elements (La/Yb > 10, Nb/Y > 0.4) and exhibit low Ba/La and B/La, approaching compositions of oceanic basalts (Figs. 3, 4). Melt inclusions from Arenal are broadly intermediate in composition between those from Nicaragua and those from Guatemala and Irazú Volcano.

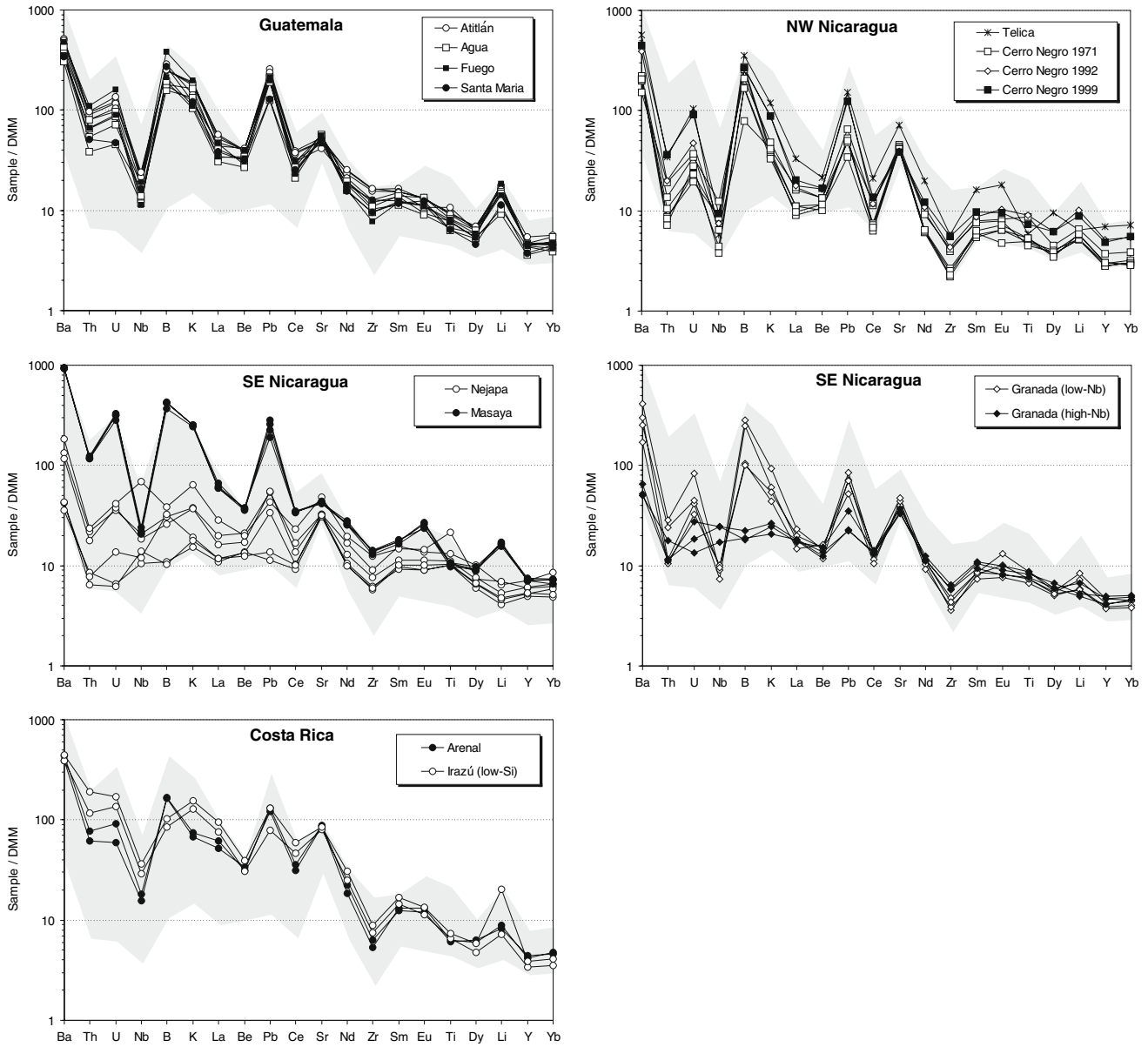

Fig. 3 Incompatible trace elements in melt inclusions normalized to the composition of depleted MORB mantle (DMM; Salters and Stracke 2004). *Shaded field* illustrates the entire compositional range of the melt inclusions from Central America

Melt inclusions from Nicaragua show strong compositional variability over short distances along the volcanic front and also on the scale of single samples. Cerro Negro Volcano displays the greatest slab signal (e.g. Ba/La) along the entire Central American Volcanic Arc. This signal is however very weak just 60 km away from Cerro Negro in melts from Nejapa lineament and also in the Granada area further southeast. These melts have very low B/La < 1, Ba/La < 40 and in this respect are similar to melts from Irazú Volcano (Fig. 4). Irazú melts, however, have greater LREE enrichment than the melts from Nejapa and Granada, which display smooth EMORB-like patterns of incompatible elements with the exception of pronounced enrichments in Ba, Pb and Sr (Fig. 3). A distinctive feature of these melts is relative enrichment in Nb over other incompatible elements (Nb/La up to 2). These Nb-rich melts also have extraordinarily high Nb/U ratios of up to 100 (Fig. 4).

Substantial compositional heterogeneity among Nicaraguan magmas is also evident from the large scatter of trace element concentrations in melt inclusions from single samples. Up to one order of magnitude variations in trace element concentrations and ratios of highly incompatible elements are observed for inclusions from Cerro Negro, Nejapa and Granada (Figs. 3, 4). The Granada melt inclusions are particularly interesting in that at least two contrasting groups of melts were sampled. Inclusions of

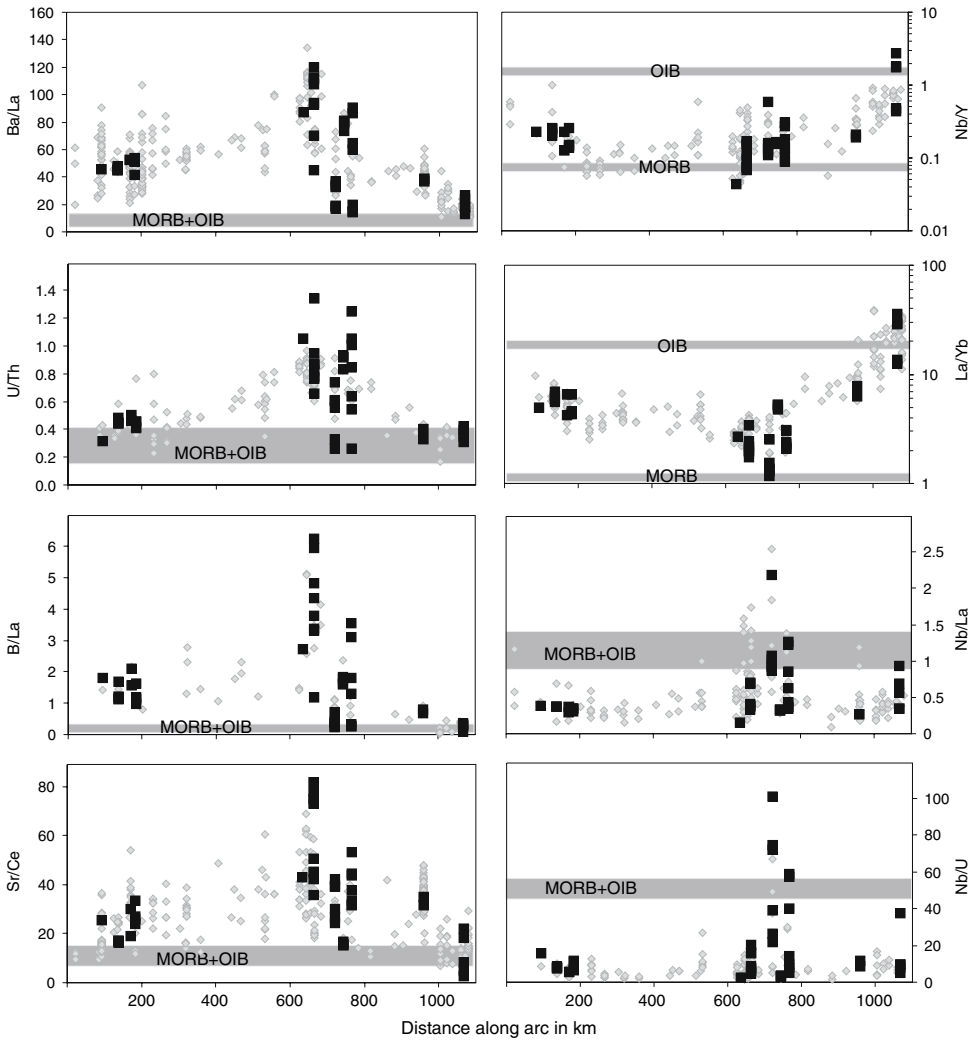

Fig. 4 Characteristic ratios of incompatible trace elements in melt inclusions plotted versus distance along the arc. *Filled symbols* denote data from this study, *small gray diamonds* denote compositions of primitive to moderately evolved whole rocks with $SiO_2 < 54$ wt%. *Horizontal lines* illustrate typical trace element ratios in mid-ocean-ridge basalts (MORB) and ocean-island basalts (OIB) (Chaussidon and Jambon 1994; Hofmann 1988; Sun and McDonough 1989)

one group (Cerro-Negro-like) in relatively low-Fo olivines (Fo_{79}) have typical arc-type patterns of trace elements with low Nb and Zr concentrations and strong enrichment in fluid-mobile trace elements (K, B, U, Pb and also H_2O). Melts of the other group (Nejapa-like), which occur in more Fo-rich olivines (up to Fo_{87}), have much lower concentrations of fluid-mobile trace elements but higher Nb, Zr and Hf. These two distinctive groups of inclusions from Granada are henceforth referred to as low-Nb (LNB) and high-Nb (HNB) groups.

Volatiles

Water concentrations range from <0.5 to ~5 wt%, which is within the range of previously reported data (Benjamin et al. 2007; Roggensack 2001a, b; Roggensack et al. 1997; Sisson and Layne 1993; Wade et al. 2006; Walker et al. 2003), but extends the range to more Fo-rich olivines (Table 1, Fig. 5). Many melt inclusions from olivine phenocrysts with Fo > 80 are relatively high in water (2–5 wt%), whereas most of those from more evolved olivine phenocrysts (Fo < 80) have <2 wt% H_2O and therefore have likely experienced degassing before trapping (Fig. 5). When inclusions in olivine with Fo > 80 are compared, the highest H_2O concentrations (>4 wt%) were found in the 1971 A.D. eruption of Cerro Negro (similar to those previously reported at Cerro Negro; Roggensack 2001a; Roggensack et al. 1997), in low-Nb type inclusions from Granada and in a single inclusion in high-Fo olivine from the 1963 A.D. eruption of Irazú. Inclusions from Guatemala and high-Nb inclusions from Granada have intermediate H_2O concentrations (2–4 wt%). Inclusions from Nejapa, all of which have high Nb, have the lowest H_2O contents (≤2 wt%). Maximum H_2O/K_2O ratios in the primitive inclusions are highest in Nicaragua (H_2O/K_2O up to ~25, excluding 1 point) and substantially lower in Guatemala and Costa Rica.

Maximum sulfur concentrations in the melt inclusions from all segments are 2,000–2,500 ppm. Higher

concentrations (up to 4,000 ppm) were reported for Costa Rican volcanoes (Benjamin et al. 2007; Wade et al. 2006). Sulfur concentrations in melt inclusions tend to decrease with decreasing Fo of olivine and increasing SiO_2 and K_2O of the inclusions, which suggests magmatic sulfur degassing occurred in conjunction with crystal fractionation (Benjamin et al. 2007; Sisson and Layne 1993; Wade et al. 2006). Thus, the measured concentrations should be considered as minimum estimates for parental magmas, which may be even more sulfur-rich than the melt inclusions trapped in variably evolved olivines. Ratios of S/K_2O exhibit clear regional variations with the highest of up to ~1 in Nicaragua and decreasing down to 0.2–0.4 in Guatemala and Costa Rica, which is apparently due to large regional variations in K_2O content.

Chlorine concentrations in the melt inclusions range from 300 ppm (Nicaragua) up to 2,500–3,500 ppm (in low-Fo olivines from Costa Rican volcanoes) and exhibit a general increase with decreasing Fo of the olivine (Figs. 5, 6). There are also good positive correlations between Cl content and incompatible element abundances (e.g. K_2O) in suites of co-genetic inclusions indicating no or only weak Cl degassing during the early stages of fractionation of Central American magmas (Benjamin et al. 2007; Sisson and Layne 1993; Wade et al. 2006). Cl/K_2O ratios measured in inclusions hosted by primitive olivines can therefore be informative of their parental melts. Distinctively high Cl/K_2O (0.2–0.4) is typical for inclusions from Nicaragua (except degassed inclusions in evolved olivines from Masaya) and also for inclusions from Arenal Volcano in Costa Rica (Cl/K_2O up to 0.8; Wade et al. 2006). Potassium-rich inclusions from Guatemala and Irazú Volcano have relatively low Cl/K_2O (0.07–0.15) although their absolute Cl concentrations are higher than that in Nicaragua.

The majority of melt inclusions from the Central America have fluorine concentrations 100–800 ppm with up to ~3,000 ppm in andesitic inclusions in low-Fo olivines from Irazú (Figs. 5, 6). Fluorine concentrations increase with decreasing Fo number of the host olivine and strongly correlate with a number of incompatible elements (e.g. K_2O, Be, La). Melts from Nicaragua generally have the lowest F concentrations, melts from Guatemala and Arenal Volcano are moderately enriched, and melts from Irazú have the highest F concentrations at a given olivine composition. The highest F/K_2O ratios were found in low-K_2O melts from Nejapa and Granada.

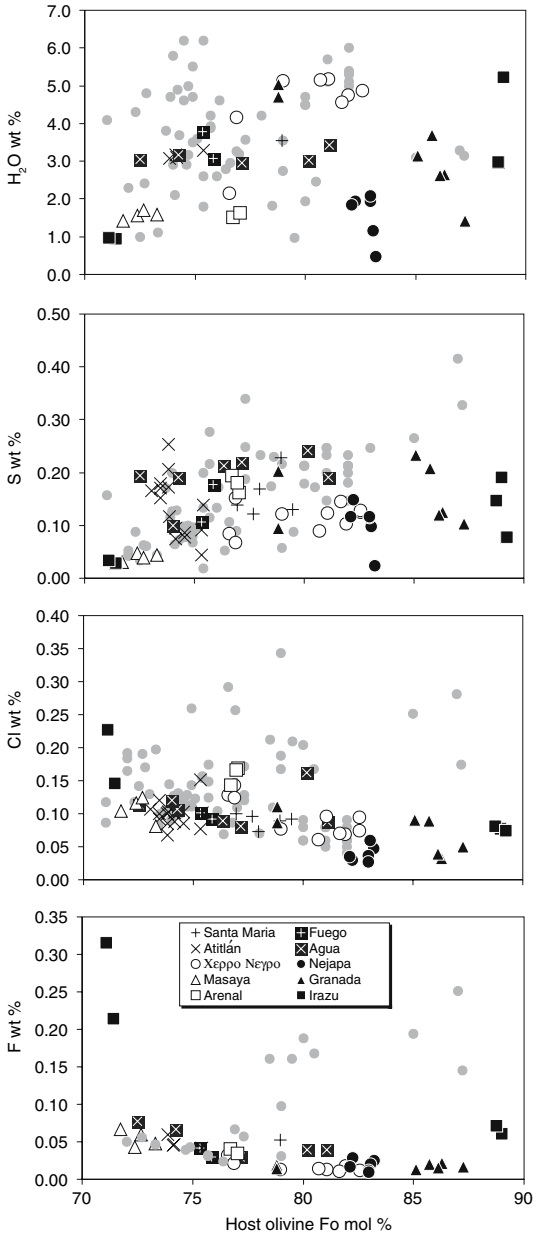

Fig. 5 Concentrations of volatile components in melt inclusions plotted versus composition of host olivines. *Small gray symbols* are previously published data on volatiles in olivine-hosted inclusions from Central America (Benjamin et al. 2007; Harris and Anderson 1984; Roggensack 2001a, b; Roggensack et al. 1997; Sisson and Layne 1993; Wade et al. 2006; Walker et al. 2003). Inclusions in low Fo olivine (Fo < 70 mol%) are not shown

Parental melts

For comparison of volatile and incompatible element concentrations of melt inclusions trapped in olivine at varying degrees of magmatic fractionation and for assessing the possible compositions of parental, mantle-derived melts, we corrected the data for passive enrichment during fractional crystallization by adding olivine until equilibrium was reached with mantle olivine of Fo_{91} (Kelley et al. 2006; Portnyagin et al. 2007). For this calculation, we assume that the only changes to the melt compositions

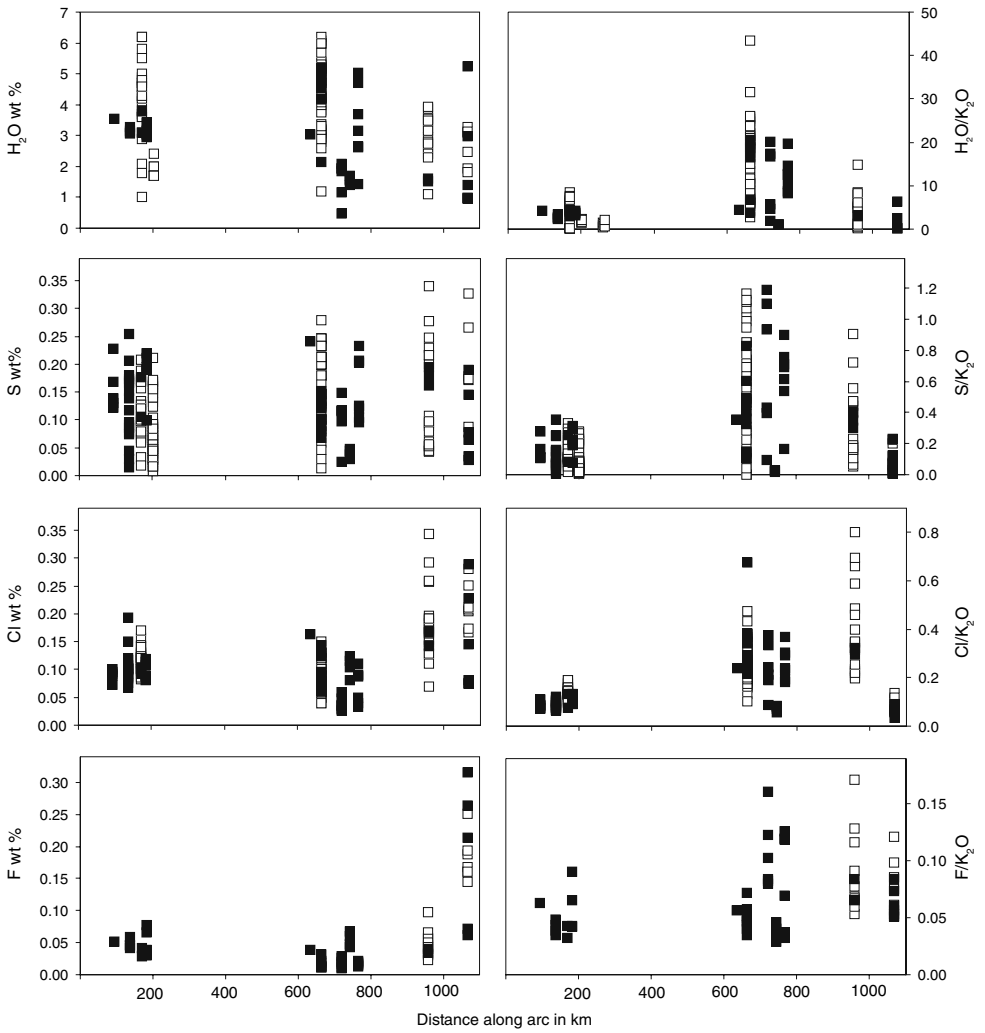

Fig. 6 Along-arc variations in concentrations of volatile components in melt inclusions and volatile/K_2O ratios. *Filled symbols* are data of this study, *open symbols* denote data from the literature (see Fig. 5 for sources)

result from fractional crystallization of olivine. Since pyroxene and probably plagioclase were most likely also liquidus phases of melts in olivines with Fo < 80, some major element contents (e.g. Ca, Al, Fe) cannot be accurately estimated in the parental melts with this method. Incompatible trace elements however are less sensitive to the modal crystallizing assemblage, and concentrations of trace elements normalized to Fo_{91} provide a better assessment of parental melt compositions than uncorrected melt inclusions or compositions corrected to certain concentrations of MgO or SiO_2 (see Portnyagin et al. 2007 for details of uncertainties).

The applied normalization to olivine with Fo_{91} is straightforward for incompatible elements. Their concentrations decrease proportionally to the amount of added olivine, which does not contain appreciable quantities of incompatible elements. Concentrations of selected major and trace elements in the estimated parental melts are shown in Table 2 (see online supplement for complete data set). For this calculation, we used the inclusions trapped in the most magnesian olivines for each sample (indicated in Table 2). For Granada, where we distinguish two geochemically different groups of melts, we calculated the parental melts for each group separately.

Behavior of volatile components is more complex during magmatic evolution, because a significant amount can be lost through degassing from magmas during fractionation, as demonstrated previously for Fuego, Cerro Negro and Arenal Volcanoes (Benjamin et al. 2007; Roggensack et al. 1997; Sisson and Layne 1993; Wade et al. 2006), and is also evident from our data. Our goal was therefore to select the least degassed inclusions from the entire data set in order to get the most reliable estimates for parental magmas.

The applied approach is illustrated in Fig. 7 using the extensive data set available for Cerro Negro inclusions (this study and Roggensack 2001a; Roggensack et al. 1997). First, we assumed that parental melt for the melt inclusions trapped in olivine from one volcano evolved exclusively due to crystal fractionation and degassing. If

Table 2 Estimated compositions of parental melts

Arc segment	Guatemala				Nicaragua				Costa Rica	
Volcano	Santa Maria	Atitlán	Fuego	Agua	Cerro Negro	Nejapa	Granada (low-Nb Group)	Granada (high-Nb Group)	Arenal	Irazú
Olivine Fo range	77–79	75–76	75–77	77–81	79–83	82–83	79–86	86–87	76–79	88–89
SiO_2 (wt%)	51.2	51.4	49.2	48.9	46.9	46.2	46.9	47.3	49.3	50.2
TiO_2 (wt%)	0.83	0.99	0.74	0.78	0.57	1.12	0.79	0.94	0.82	0.80
FeO (wt%)	9.0	10.3	10.7	9.4	11.0	11.7	11.2	9.3	10.8	8.0
Na_2O (wt%)	2.8	2.8	2.8	2.9	1.4	1.8	1.7	1.8	2.0	2.4
K_2O (wt%)	0.85	0.89	0.61	0.68	0.21	0.15	0.32	0.13	0.38	0.87
H_2O/K_2O	4.3	3.5	7	4.2	25	20	13	20	8	6.3
S/K_2O	0.3	0.4	0.3	0.3	1.0	1.2	0.7	0.9	0.9	0.23
Cl/K_2O	0.09	0.09	0.14	0.11	0.30	0.24	0.24	0.28	0.32	0.08
F/K_2O	0.06	0.04	0.04	0.06	0.05	0.11	0.04	0.12	0.07	0.07
H_2O (wt%)	3.7	3.1	4.3	2.9	5.4	3.0	4.2	2.7	3.1	5.5
S (wt%)	0.26	0.36	0.18	0.20	0.21	0.18	0.22	0.12	0.34	0.20
Cl (wt%)	0.08	0.08	0.09	0.07	0.05	0.04	0.08	0.04	0.12	0.07
F (wt%)	0.05	0.04	0.02	0.04	0.01	0.02	0.01	0.02	0.03	0.06
B (ppm)	12.7	13.4	10.0	9.2	9.2	1.2	8.8	1.0	7.6	4.8
Zr (ppm)	59	79	48	71	19	49	26	42	36	56
Y (ppm)	12	15	15	13	10	19	13	16	14	13
Nb (ppm)	2.7	3.0	1.9	2.6	1.2	4.1	1.5	4.1	2.7	5.9
Ba (ppm)	318	358	330	342	190	88	272	59	384	429
La (ppm)	7.0	8.0	6.3	7.5	2.3	3.1	3.5	3.7	10.2	17
Th (ppm)	0.55	0.85	0.71	0.52	0.12	0.16	0.20	0.16	0.74	1.8
U (ppm)	0.17	0.38	0.33	0.23	0.10	0.09	0.19	0.08	0.27	0.6

Notes. Major and trace elements in parental melts represent mean values obtained for a suite of cogenetic inclusions from every sample after recalculating the compositions to be in equilibrium with olivine Fo_{91}. "Olivine Fo range" indicates the range in Fo of the host olivines for the inclusions used in determining the parental melt compositions. The volatile/K_2O ratios for parental melts were estimated from populations of variably degassed co-genetic inclusions (see Fig. 7) and generally represent maximum values for H_2O/K_2O, S/H_2O and Cl/K_2O and mean estimates for F/K_2O. Absolute concentrations of volatiles in parental melts are calculated from the volatile/K_2O ratios and the mean K_2O content in parental melts. Literature data were also used for Arenal, Irazú, Fuego, Cerro Negro and Pacaya (Benjamin et al. 2007; Roggensack 2001a, b; Roggensack et al. 1997; Wade et al. 2006; Walker et al. 2003;; Sisson and Layne 1993)

only crystal fractionation has occurred, ratios of volatile components to incompatible lithophile elements (e.g. K_2O) should remain constant. If degassing has taken place, these ratios will decrease due to partitioning of the volatile component into the fluid phase. In the Cerro Negro melt inclusions, H_2O, S and CO_2 decrease with increasing K_2O, exhibiting clear degassing trends. Chlorine concentrations increase with increasing K_2O but Cl/K_2O decreases, suggesting partitioning of some amount of Cl into fluid phase. For these volatiles, the maximum measured ratios of volatiles to K_2O (H_2O/K_2O, S/H_2O, Cl/K_2O and CO_2/K_2O) should be closest to the initial ratio in the parental melt. Fluorine concentrations in melts increase proportionally to K_2O concentrations suggesting little or no degassing of fluorine during fractionation. Therefore, mean F/K_2O gives us the best idea of the mean ratios in the parental melt. If the volatile to K_2O ratios in the parental melts is known or can be assumed, it is possible to estimate the absolute concentrations of volatiles from independently estimated K_2O contents in the parental melt.

Trends similar to those in Fig. 7 were also evident for Fuego Volcano in Guatemala (Sisson and Layne 1993) and Arenal (Wade et al. 2006) and Irazú (Benjamin et al. 2007) Volcanoes in Costa Rica and appear to be typical for Central America. Therefore, we can extend this approach to other, more limited data sets of melt inclusion compositions. We have estimated the maximum H_2O/K_2O, S/K_2O, Cl/K_2O and mean F/H_2O for all inclusions from every volcano and then calculated absolute volatile abundances in parental magmas from the mean K_2O concentrations in them (Table 2). Literature data were also used where available (Arenal, Fuego, Cerro Negro, Pacaya, Irazú).

It should be noted that the applied approach provides no guarantee that estimated ratios were not affected by earlier degassing that was not recorded in the melt inclusions. Therefore, the reported volatile contents and ratios should

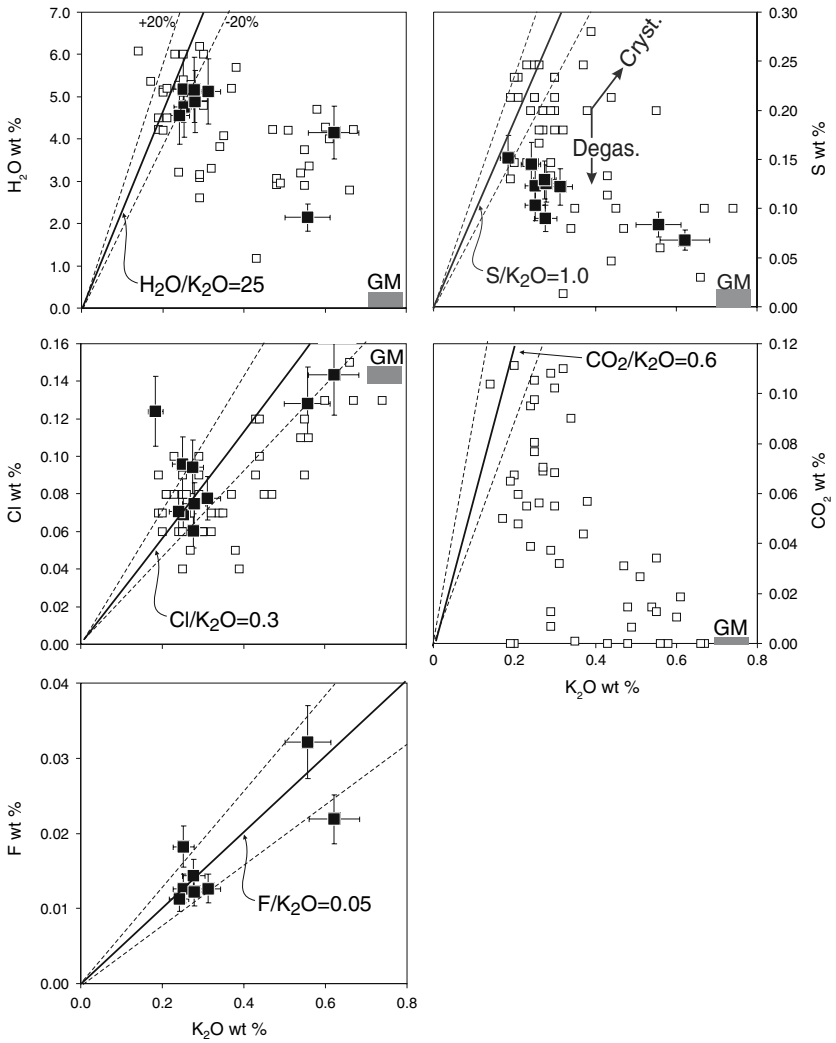

Fig. 7 Water, S, Cl, CO_2 and F concentrations in Cerro Negro melt inclusions plotted versus K_2O content. *Filled symbols* are data from this study, *open symbols* from Roggensack (2001a), Roggensack et al. (1997), 'GM' labeled box indicates groundmass composition of the host tephra. Note decreasing H_2O, S and CO_2 concentrations with increasing K_2O, which indicates crystallization accompanied by extensive magmatic degassing of these volatiles. Chlorine concentrations increase with increasing K_2O but Cl/K_2O decreases slightly indicating that some Cl partitions into the fluid phase. Maximum H_2O/K_2O, S/H_2O, CO_2/K_2O and Cl/K_2O ratios are believed to be closest to the parental melt composition. Fluorine concentrations increase nearly proportionally to K_2O, which implies that significant F degassing does not occur during crystallization. Therefore F/K_2O may be informative of parental melt composition. *Solid lines* illustrate constant volatile/K_2O ratios, which are assumed to be characteristic for parental melt of this volcano. *Dashed lines* bracket ±20% uncertainty of the parental melt estimates. *Error bars* correspond to 15% relative standard deviation (RSD) for volatiles and 10% RSD for K_2O

be considered as minimum values for true parental melts. For this reason, we did not include data for Masaya Volcano in our compilation, because the inclusions were trapped in evolved olivines and H_2O, S and Cl had already significantly degassed, when compared to inclusions in more forsteritic olivines from Nicaragua or Guatemala (Fig. 5). The other disadvantage of this approach is that it does not account for possible variations of volatile contents and ratios to incompatible elements in parental magmas at a single locality. In light of large geochemical heterogeneity of inclusions from some samples, volatile heterogeneity is also to be expected (Fig. 3). This uncertainty cannot be quantitatively accounted for at present and requires better statistics on both volatile components and other incompatible elements in melt inclusions.

Discussion

What are the causes of incompatible trace element variations along the arc?

Incompatible trace elements measured in melt inclusions exhibit large regional variations, which agree well with the

geochemical zoning observed in the whole rocks (Fig. 4). Therefore the conclusions drawn from melt inclusion and whole rock geochemistry are similar. Both whole rock and melt inclusion compositions change systematically along the arc. The highest Ba/La, B/La, U/Th and Sr/Ce ratios are observed in Nicaragua. The ratios decrease southwards into Costa Rica, reaching very low values similar to oceanic basalts at the southernmost Irazú Volcano, and northwards into Guatemala, reaching intermediate values (Fig. 4). As pointed out by many authors, the large variation in highly incompatible-element ratios in the Central American lavas can be attributed to variable fluid flux from the subducting Cocos Plate and also to multi-stage and/or multi-component processes of mantle enrichment (Carr et al. 1990; Eiler et al. 2005; Leeman et al. 1994; Patino et al. 2000).

The sedimentary pile on the subducting Cocos Plate consists of two units: the lower consists of carbonates and the upper of hemipelagic sediments (see overview in Patino et al. 2000). Although both sedimentary units have high U/Th and Ba/La (Figs. 4, 8a), the hemipelagic sediments have high U concentrations and U/La and low Ba/Th compared to the carbonates, making it possible to distinguish between the two sedimentary input components (Fig. 8b). As shown by Patino et al. (2000), Ba/Th and U/La form negative arrays for lavas from some volcanoes in Central America (for example see field for Telica in Fig. 8b), indicating that varying proportions of the two sedimentary units are involved in the magma generation process. Cerro Negro and low-Nb Granada melt inclusions extend to high Ba/Th at low U/La indicating an important role for carbonate sediments, whereas Masaya melt inclusions trend towards higher U/La at low Ba/Th, indicative of the presence of a hemipelagic component in their magma genesis (Fig. 8b). Most of the melt inclusion data, however, have relatively low Ba/Th, U/La and U/Th and cluster near depleted MORB-source mantle (DMM). Melt inclusions with little contribution of U- and Ba-rich component(s) most likely derived from subducted sediments include all but one data point from Guatemala, some data from all volcanoes in Nicaragua except Masaya and data from both studied Costa Rican volcanoes.

Additional important questions concerning the genesis of Central American magmatism that can be addressed with trace element geochemistry are whether other portions of the subducting slab also contribute to magma genesis and whether slab components that are added to the mantle wedge have fluid- or melt-like properties. Ratios of elements that are not highly fluid mobile in arc systems, such as the REE and HFSE, can help evaluate the role of slab components with melt-like properties. On a diagram of La/Sm versus Ba/La (Fig. 8c), melt inclusions from central Nicaragua (Cerro Negro, Granada and Nejapa) form a

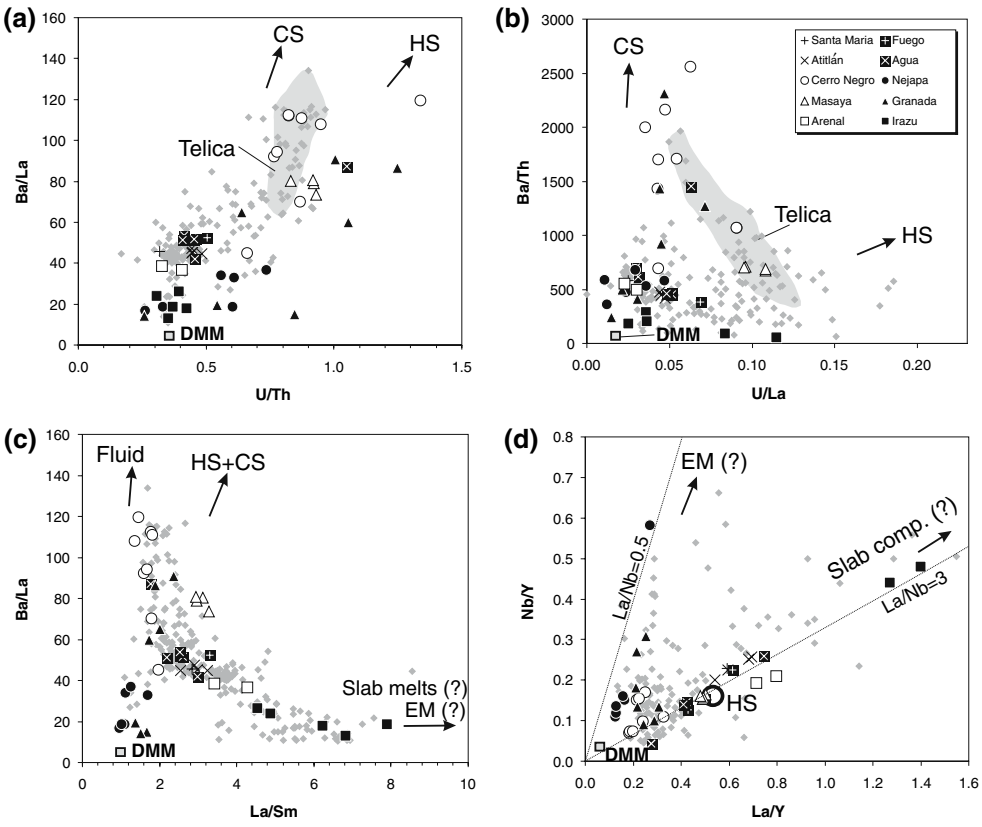

Fig. 8 Variations of incompatible trace element ratios in the melt inclusions. *Small gray symbols* illustrate compositions of primitive to moderately evolved rocks from Central America ($SiO_2 < 54$ wt %). *Shadowed field* encloses compositions of Telica Volcano rocks (Patino et al. 2000). CS and HS labels indicate compositions of hemipelagic and carbonate sediments, respectively, from the DSDP site 495 (Patino et al. 2000); DMM is the composition of depleted MORB mantle source (Salters and Stracke 2004); EM–Nb-enriched (OIB-like?) mantle

nearly vertical trend at low La/Sm. Nejapa and high-Nb Granada inclusions have the lowest Ba/La ratios, whereas Cerro Negro and low-Nb Granada inclusions extend to the highest Ba/La ratios. Taken together with the discussion of Ba/Th versus U/La systematics above, this trend could be explained by the addition of variable amounts of Ba-rich (derived from subducting carbonate sediments) fluid, most clearly seen in Cerro Negro and low-Nb Granada melt inclusions, to a relatively depleted (DMM) mantle wedge, represented most closely by high-Nb Granada and Nejapa melt inclusions. Oxygen isotope data also indicate substantial variation in the amount of slab components involved in the sources of Nicaraguan magmas (Eiler et al. 2005). Cerro Negro magmas, however, have lower $\delta^{18}O$ than those from Nejapa and Granada, opposite of what is expected for a sediment-derived component with high $\delta^{18}O$. This observation suggests that the slab-component (fluid), carrying the strong sediment signature to the Cerro Negro magma sources, contains only a very small mass fraction of sedimentary material. The bulk of the slab component must be largely derived from the lower oceanic crust or serpentinites (both of which have low $\delta^{18}O$; Eiler et al. 2005), possibly scavenging Ba from overlying sediments as it migrates upwards.

Melts from Guatemalan Volcanoes and Masaya Volcano in Nicaragua have intermediate Ba/La and La/Sm and high $\delta^{18}O$ above mantle values compared to similarly Ba-rich Cerro Negro melts (Fig. 8 a, b). These systematics are difficult to reconcile with a single slab-component model (Eiler et al. 2005). A more plausible explanation could be that another Ba- and LREE-rich and high-$\delta^{18}O$ crustal component is involved in magma genesis beneath Guatemala. The absolute amount of this crustal component in the sources of Guatemalan magmas may be even larger than in Nicaragua, and its geochemical features (high $\delta^{18}O$) are more compatible with derivation of the fluid from altered oceanic crust and/or subducting sediments rather than serpentinite (Eiler et al. 2005). The origin and provenance of this component, which also has relatively low B/Be and $^{10}Be/^{9}Be$ (Leeman et al. 1994; Morris et al. 1990), is unclear and represents one of the most fundamental problems of Central American arc volcanism. This component could be a sediment-derived melt (Eiler et al. 2005), possibly solidified and aged in the mantle wedge and melted later as a result of fluid fluxing from deeper portions of the subducting slab (Leeman et al. 1994; Patino et al. 2000), or alternatively melt from the upper continental crust with high La/Sm and low Ba/La (Carr et al. 1990).

The Costa Rican magmas are characterized by the highest La/Sm and La/Yb ratios (greatest LREE enrichment) but among the lowest Ba/La, Ba/Th and U/Th ratios, suggesting either involvement of an enriched mantle wedge (Abratis and Wörner 2001; Carr et al. 1990; Feigenson et al. 2004) or a melt-like component derived from the magmatic portion of the downgoing slab (Fig. 8). Although the Guatemalan melts have intermediate La/Sm, Ba/La, U/La and Ba/Th compared to Costa Rican and some Nicaraguan (Cerro Negro and low-Nb Granada) melts, the lower, mantle-like $\delta^{18}O$ of the Costa Rican magmas precludes mixing of the Costa Rican melt-like slab component with the Nicaragua fluid-like slab component to generate the composition of the Guatemalan melts. Our conclusion from these observations is that the along arc geochemical variations in Central America reflect involvement and mixing of multiple distinct crustal (from subducting and/or overriding plates) and mantle (wedge and subducting slab, e.g. serpentinite) components, with slab components having both fluid- and melt-like characteristics, and variable extents of partial melting of the metasomatized mantle wedge (Eiler et al. 2005).

Two types of Nb enrichment in Central America

The earlier discussion about different slab components contributing crustal signatures to the Central American magmas is also relevant for reconciling a dilemma about mantle versus slab source control on HFSE (Nb, Zr) and LREE enrichment in lavas (Abratis and Wörner 2001; Carr et al. 1990; Feigenson et al. 2004; Leeman et al. 1994). To address this problem, we plotted compositions of primitive melt inclusions from all segments of the arc in coordinates Nb/Y versus La/Y (Fig. 8d). This diagram clearly demonstrates the existence of two distinctive compositional trends of coupled enrichment in Nb and La in the Central American magmas, both converging at very low Nb/Y and La/Y similar to the depleted MORB source (Salters and Stracke 2004). Melt inclusions from Nejapa, high-Nb group from Granada and some Cerro Negro melts (all from central Nicaragua) form one trend, which points to the source component with low La/Nb $\sim$ 0.5. Melt inclusions from Guatemala, Costa Rica and the remaining from Nicaragua (Masaya, low-Nb Granada group and some from Cerro Negro) form the other trend toward a Nb- and La-rich component with relatively high La/Nb $\sim$ 3.

The low La/Nb observed in some Nicaraguan melts is unusual for subduction-related magmas and more typical for incompatible-element-enriched oceanic basalts (Hofmann 2003; Sun and McDonough 1989). The simplest explanation for Nb enrichment in Nicaraguan magmas is involvement of HFSE-rich peridotite (or pyroxenite; Sobolev et al. 2007) similar to the source of oceanic island basalts and possibly imbedded in depleted DMM-like matrix (Carr et al. 1990; Walker et al. 1990). The Nb-rich basalts in Nicaragua however have unusually high Nb/U ratios (up to 100, Fig. 4) compared to most OIB with Nb/U

of 47 ± 10 (Hofmann 2003). Nb/U ratios exceeding 100 have been found in Canary Island basalts, possibly reflecting contamination of these intraplate magmas with melts from amphibole/phlogopite-rich veins located in the lithosphere (Lundstrom et al. 2003). Nb-enriched lithologies can also be formed during dehydration and/or partial melting of slab material (Garrido et al. 2005; Ionov and Hofmann 1995).

Unlike Nicaragua, Nb-enrichment in Guatemala and Costa Rica is coupled with strong LREE enrichment (Fig. 8 c, d). The pronounced negative Nb anomaly in normalized trace element spectra of these melts (Fig. 3) points to subduction-related metasomatism. Noteworthy is also the close coincidence of La/Nb (~3) in Guatemalan melts and subducting hemipelagic sediments. Sediment melts can therefore explain some Nb-enrichment in the magma source beneath Guatemala as proposed recently for southern Kamchatka (Duggen et al. 2007).

Irazú melts exhibit the highest La/Y and Nb/Y along the high-La/Nb trend, which can be in principle explained by involvement of low-degree melts from subducting sediments leaving eclogitic residue. This hypothesis however is not consistent with existing Pb-isotope data indicating strong HIMU signature in Costa Rican magmas, closely resembling Galápagos-type mantle (Abratis and Wörner 2001; Feigenson et al. 2004) or crustal material. On the basis of this data, a reasonable explanation for the peculiar geochemical features of the Costa Rican volcanic rocks can be involvement of partial melts from the subducting slab (i.e. Galápagos hotspot track), leaving a rutile-bearing eclogitic residue to explain high LREE and La/Nb. Alternatively, the Galápagos crustal signature could be inherited from Galápagos-related complexes formerly accreted to the Costa Rican fore-arc, which were eroded and then melted beneath the arc (Goss and Kay 2006). These two hypotheses can probably be sorted out with the help of detailed Pb-isotope studies but in essence they both coincide in the principle conclusion that the enrichment in HFSE and LREE is derived from the subduction input and not intrinsic to the mantle in the wedge.

Test of water-fluxed melting beneath Central America

Most previous studies of Central American arc magmatism assumed that mantle melting is fluxed by water-rich fluids or melts from the subducting plate (Carr et al. 1990; Eiler et al. 2005; Patino et al. 2000; Walker et al. 1990), although this has not yet been directly demonstrated. A crucial test for the viability of water-fluxed melting is the existence of an inverse correlation between water content and incompatible element content in the primary magmas, which implies open system melting promoted by water addition to the source (Stolper and Newman 1994). The best candidates for indices of partial melting are Na, Ti, Y and HREE. The abundances of these elements in mantle sources are relatively constant, and their abundances are either high in the mantle wedge and thus not substantially affected by the addition of small amounts of fluids (e.g. Na) or low in slab-derived fluids and melts (e.g. Ti, Y, HREE). Covariations between H_2O, TiO_2, Y and Na_2O in the inferred parental Central American magmas are shown in Fig. 9.

First-order observation from our data is that H_2O in parental melts does correlate inversely with TiO_2, Y and Na_2O. Squared correlation coefficient for linear regressions range from 0.43 (H_2O vs Na_2O) to 0.65 (H_2O vs TiO_2) and are significant at the 99% confidence level. Thus, our principle conclusion is that melting beneath all parts of the Central America arc is indeed triggered by addition of water-bearing components. Similar correlations can also be produced by mixing of incompatible-element-depleted, water-rich melts (e.g. Cerro Negro) with incompatible-element-enriched water-poor melts (e.g. Guatemalan rear-arc). This however does not explain other geochemical features of the Central American magmas, which require several regionally different compositional components as discussed above (see Fig. 8).

In this work we did not attempt a fully quantitative modeling of flux melting for the Central America magmas but made some preliminary estimates of the thermal conditions of melting and possible compositions of mantle sources, which govern productivity of water-fluxed melting and are crucial for correct determination of degrees of partial melting (Kelley et al. 2006; Portnyagin et al. 2007). We did our modeling following the approach and equations of water-fluxed melting from Portnyagin et al. (2007), which assumes simple batch melting with constant partition coefficients and uses parameterization of hydrous melting after (Katz et al. 2003).

First, we determined that most compositions of the Central American parental melts are bracketed by the model compositions of partial melts generated by water-fluxed melting of depleted MORB mantle (DMM; Salters and Stracke 2004) in spinel facies at temperatures from +25 to –50°C of the dry peridotite solidus (DPS) (Fig. 9). This result is in agreement with previous estimates (Portnyagin et al. 2007) and suggests that (1) mantle wedge beneath the Central American volcanic belt is relatively cold compared to mantle source regions beneath mid-ocean-ridges, back-arcs and possibly intra-oceanic arcs (Portnyagin et al. 2007), (2) nearly all melting is water-fluxed beneath Central America, and (3) dry decompression melting, which occurs at temperatures above the dry peridotite solidus, is limited to several percentage and is clearly less important than water-fluxed melting.

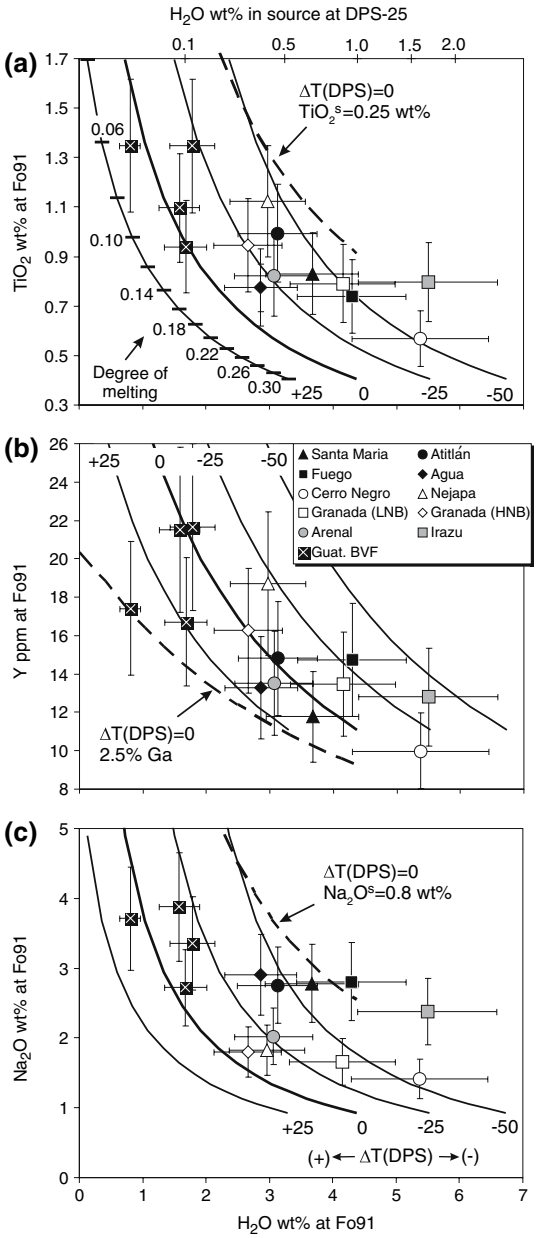

Fig. 9 Correlations of H_2O and **a** TiO_2, **b** Y and **c** Na_2O content in ▶ inferred parental melts. Compositions of the Guatemala rear-arc parental melts were calculated using data from Walker et al. (2003) and are shown for comparison with volcanic front samples. *Error bars* correspond to 20% RSD. *Solid curves* are modeled compositions of partial melts (from 2 to 30% melting with 2% increments as indicated in **a**) produced during water-fluxed melting of depleted MORB source (DMM; Salters and Stracke 2004) in spinel facies at different temperatures (°C) above and below the Dry Peridotite Solidus (DPS). Amount of water in mantle source calculated at ΔT(DPS) = –25°C (or 25°C below the DPS) is shown at the *top* of diagram (**a**). *Dashed curves* illustrate melting trajectories at ΔT(DPS) = 0 (or simply at DPS) with slightly different input parameters: **a** TiO_2 = 0.25 wt% in source instead of 0.133 wt% in DMM; **b** in presence of 2.5% garnet in the source (bulk D^Y = 0.2 instead of D^Y = 0.095 in spinel facies); **c** Na_2O = 0.8 wt% in source instead of 0.29 wt% in DMM. Modeling was done following equations and approach by Portnyagin et al. (2007). Partition coefficients used were the same as in Kelley et al. (2006). Note that position of data points changes relative to modeled curves in different coordinates, which indicates that DMM is not an appropriate source for all magmas in Central America and some melting could take place in the garnet stability field

Looking at the data in detail, the position of individual data points and the whole data array relative to the model melt compositions at different temperatures are not constant in the different diagrams in Fig. 9. For example, H_2O–Y variations suggest temperatures near DPS, while H_2O–TiO_2 and H_2O–Na_2O suggest temperatures mostly below DPS. This discrepancy can arise from the very simplified modeling approach but also can be informative of some variability of the mantle source compositions and changes in partition coefficients during partial melting. For example, if we assume that all melting in Central America took place at the DPS temperature, the deviations of melt compositions towards higher TiO_2 and Na_2O from those predicted in the model can be explained if the mantle composition varied from DMM-like (TiO_2 = 0.133 wt%) to more Ti- and Na- rich (TiO_2 up to 0.4 wt%, Na_2O up to ~0.8 wt%) (Fig. 9 a, c). This is in accordance with independent evidence of involvement of enriched mantle in magma genesis in Central America (Carr et al. 1990; Feigenson and Carr 1993; Walker et al. 1990; Patino et al. 2000) and with the incompatible-element patterns of high-Nb melts from Granada and melts from Nejapa which have low H_2O and are likely to most closely reflect the mantle wedge composition (Fig. 3). Deviations of data points towards lower Y compared to the model predictions at DPS temperature may suggest that initial mantle concentrations were lower than the DMM value (Y = 4.07 ppm) or more likely Y partition coefficient (0.095) chosen for modeling was too low. We prefer the latter explanation, which is consistent with the common presence of garnet in the sources of the Central American magmas (Feigenson and Carr 1993) and is evident from the higher normalized contents of intermediate to heavy REE (Fig. 3). According to our maximum estimate for bulk Y partition coefficient (~0.2) (Fig. 9b), the quantity of garnet in the sources of the Central American magmas did not exceed ~2.5%.

Reliable estimates of the amount of water introduced into the sources of magmas require well-justified source compositions and partition coefficients for every volcano/sample (Kelley et al. 2006; Portnyagin et al. 2007). As is evident from the discussion above, this is not an easy task for Central America magmatism and requires reconciling of effects of variable temperature, source composition and partition coefficients on the composition of mantle melts. Nevertheless, we made a rough estimate of the amount of water in the sources in order to check agreement of the mass balance of mantle and slab components predicted

from our data and $\delta^{18}O$ systematics (Eiler et al. 2005). Overall, the amounts of water in the mantle sources estimated for spinel facies DMM melted at 25°C below DPS vary from ~0.1 wt% for rear-arc melts in Guatemala up to ~1.7 wt% for Cerro Negro (Fig. 9a). The latter magmas also have the lowest $\delta^{18}O$ in Central America, and Eiler et al. (2005) estimated up to 4 wt% slab component with 50 wt% water and $\delta^{18}O$ ~0‰ in their source. We calculate from our data that Cerro Negro sources contained ~3.4 wt% slab component with 50 wt% water, in excellent agreement with the oxygen isotope data.

Trace element proxies of volatiles

In studies of arc magmatism, fluid mobile to less fluid mobile or fluid immobile trace element ratios (e.g. Ba/La, Ba/Th, U/Th, Ba/Nb) are often assumed to reflect the relative fluid contribution from the subducting slab to the mantle wedge. If this can be demonstrated to be the case for an arc, then these ratios could be used as proxies for determining water contents of magmas. This correlation can however be highly obscured due to the diversity of water-bearing components involved in arc magma generation. For example, Portnyagin et al (2007) showed that water in various primitive magmas of Kamchatka inversely correlates with TiO_2 and Na_2O but does not correlate with Ba/La or Ba/Nb. The only correlation found was between *relative* enrichment in boron and water compared to concentrations of fluid-immobile Nb and Zr. On the other hand, Wade et al. (2006) demonstrated that correlation between H_2O and Ba/La in parental melts may indeed be significant in Central America in contrast to Kamchatka. Our new data provide further insights into the relationships between trace element geochemistry and enrichment in water and other volatile elements in the Central American magmas.

As illustrated in Fig. 10, water content in the majority of parental melts of Central America strongly correlate with Ba/La and B/La ratios. Even better correlation is expected between these trace element ratios and the amount of water in the magma sources, because this amount of water is proportional to H_2O/TiO_2 or H_2O/Y, exhibiting even larger relative range than absolute H_2O concentrations (Fig. 8). Existence of this correlation can be explained if LREE-rich melt-like components required by magmas in Guatemala, Nicaragua (e.g. Masaya) and western Costa Rica had low B and Ba concentrations and were poor in H_2O. In this case elevated Ba/La and B/La ratios in magmas can be ultimately related to the magnitude of flux of Ba-, B- and H_2O-rich fluid, generating the correlations observed in Fig. 10.

The Irazú volcano, however, falls off the general Central American arrays in Fig. 10 and exhibits high H_2O at very

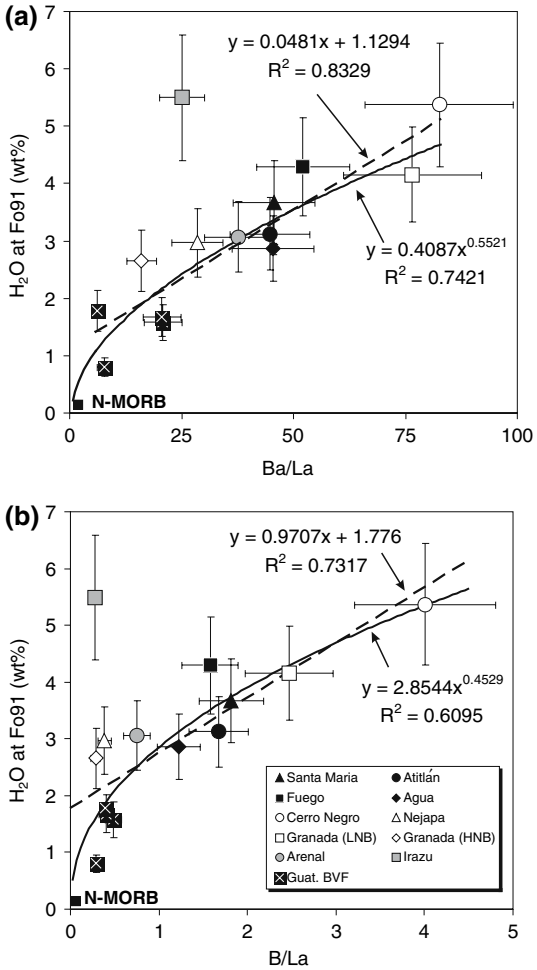

Fig. 10 Correlations of water with Ba/La and B/La ratios in the mean parental melts of the Central American volcanoes. *Error bars* correspond to 20% RSD. Data were approximated by *power* and *linear regression lines* (excluding Irazú Volcano) allowing estimate of H_2O content in parental melt from whole rock Ba/La or B/La ratios. *N-MORB* composition is shown for reference (Chaussidon and Jambon 1994; Sun and McDonough 1989)

low B/La and Ba/La. Therefore compositions of slab components involved in magma genesis in the southern part of the arc may have lower Ba/La and B/La than in northern localities, consistent with lower amounts of Ba-rich sediments on the subducting Cocos Ridge than to the north. On the other hand, the high H_2O contents suggest that the subducting hotspot track may contribute a large amount of water to arc volcanism beneath Irazú or that much of the water flux from the subducting Cocos Ridge is concentrated beneath Irazú Volcano. Clearly the composition and thermal state of the plate subducting beneath Irazú, which has been overprinted by the Galápagos hotspot, is strikingly different from normal oceanic crust entering the trench in other parts of the arc (Fig. 1) (Leeman et al. 1994; Protti et al. 1995). Although we believe that a plausible explanation for the exceptionally

high H_2O and low Ba/La in Irazú magmas can be found, our current conclusion is based on only a few data points, which need to be verified through more extensive studies of volatiles in Costa Rican magmas.

Other volatile components in parental magmas can also be traced with lithophile element ratios. Chlorine and to lesser extent sulfur concentrations in parental magmas correlate with La/Nb ratio (Fig. 11) and only weakly correlate with H_2O or Ba/La (not shown), suggesting that both S and Cl may be delivered to the mantle source via the melt-like component with high La/Nb and not with a H_2O-rich fluid. Fluorine concentrations in parental melts correlate with La/Y ratio suggesting coupled behavior of LREE and F during magma generation in subduction zones (Portnyagin et al. 2002). The slightly steeper slope defined by the data from Costa Rica can reflect a more important role for garnet in the source of these magmas resulting in elevated La/Y (Feigenson and Carr 1993).

Fluxes of volatile elements

Minimum estimate of volatile fluxes through the Central American Volcanic Arc can be obtained by combining the flux of magma to the surface with volatile abundances determined for parental magmas in this study. Because direct measurements could only be carried out on a limited number of samples, we used the previously discussed correlations between incompatible element ratios (Ba/La, La/Nb and La/Y) and volatile abundances in parental melts estimated from melt inclusions in order to constrain the volatile abundances in parental magmas throughout Central America from whole rock geochemical data (Fig. 12). From the mean calculated trace element ratios for each arc segment as given in the Centam data base of compositions of whole rocks (Carr et al. 2003), we calculated average volatile abundances for every arc segment, assuming that there was no change in the incompatible trace element ratios as a result of differentiation (Table 3). Volatile fluxes were then calculated by multiplying the average volatile content in parental magma for an arc segment with the average volcanic flux for that segment (Carr et al. 1990, 2007). We note that the volatile contents for central Costa Rica (Cordillera Central) volcanoes are poorly constrained; very large variations are predicted from the whole rock data. In particular, it is not clear how representative the high H_2O concentrations of Irazú magmas (up to 5 wt%) are for the neighboring volcanoes. Therefore, we used average Arenal and Irazú parental volatile contents for the other volcanoes in central Costa Rica and assumed an uncertainty of factor two for all estimates of volatile abundances and calculated fluxes for the segment-averaged parental melts of central Costa Rica. This uncertainty, however, only introduces a small error in the estimates of

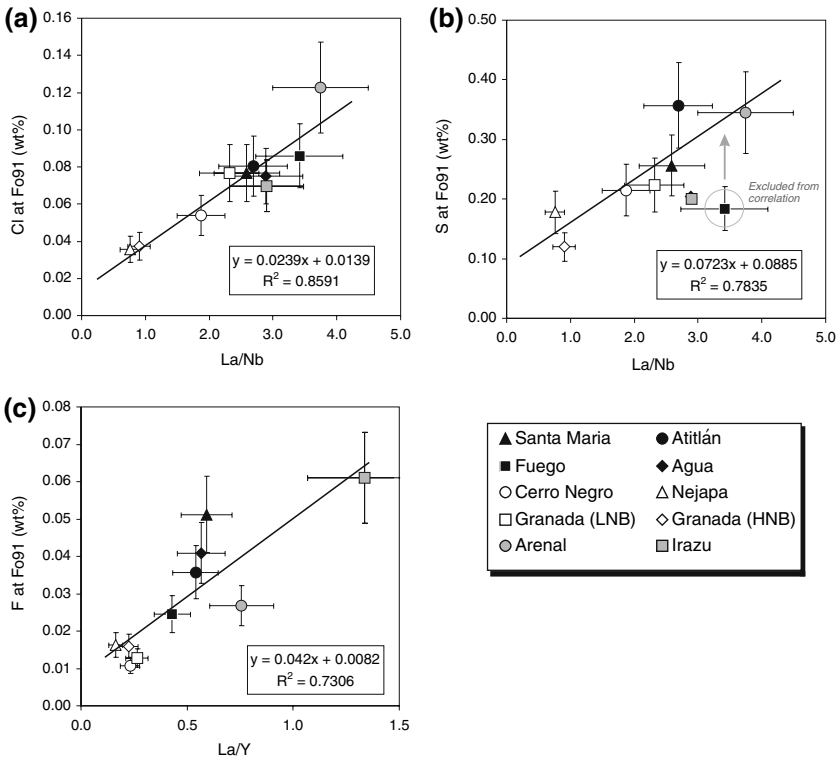

Fig. 11 Correlations of Cl, S and F with trace element ratios (La/Nb and La/Y) in parental melts. *Error bars* correspond to 20% RSD. The data were approximated by linear regressions, which allow assessment of volatile contents from whole rock trace element ratios. The regression line in **b** does not include data for Fuego volcano as it could be affected by S degassing

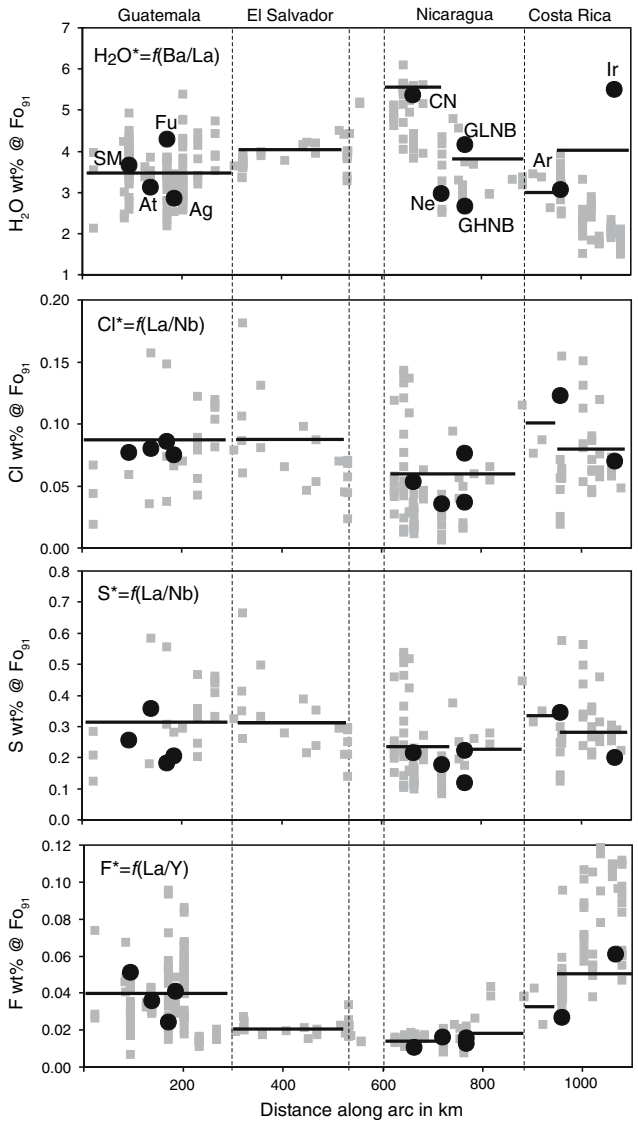

Fig. 12 Concentrations of volatile components in the Central American parental melts calculated from the compositions of primitive to moderately evolved rocks ($SiO_2 < 54$ wt%) using trace element proxies (Ba/La for H_2O, La/Nb for Cl and S, and La/Y for F). *Black dots* illustrate direct estimates based on this melt inclusion study (see Table 2 for compositions of parental melts)

the total volatile fluxes from the Central American volcanism, which are dominated by the Guatemala, El Salvador and Nicaragua segments

Considering only volcanic output, the largest fluxes of all volatiles were obtained for Guatemala and El Salvador. Water fluxes for Nicaragua and Costa Rica are similar. Sulfur, chlorine and fluorine fluxes tend to be higher in Costa Rica than in Nicaragua (Fig. 13a). Mean (normalized to the length of segments) volcanic fluxes of volatiles along the Central American Arc are 1.1×10^9 kg/m/Ma H_2O, 8.3×10^7 kg/m/Ma for S, 2.3×10^7 kg/m/Ma for Cl and 8.9×10^6 kg/m/Ma for F.

Volatile fluxes estimated above represent minimum magmatic fluxes, because they neither take into account magmatic fractionation before eruptions nor consider magmas that completely stagnate and fractionate in the lithosphere without any portion ever reaching the surface. The amount of fractionation is relatively difficult to quantify for all segments of the Central America because parental melt compositions are not well constrained on a regional scale. Using Carr et al. (2007) data for volcanic fluxes ($1.3–1.6 \times 10^{10}$ kg/m/Ma), flux of K_2O ($1.3–1.8 \times 10^8$ kg/m/Ma) in Nicaragua and assuming $K_2O \sim 0.2–0.3$ wt% in parental magmas (Table 2), we estimate that volcanic products in Nicaragua have on average 1–1.2 wt% K_2O and can originate through approximately 75–80% of crystallization of parental melts. In other words, the flux of parental magmas feeding volcanism in Nicaragua and, possibly, along the entire volcanic front in the Central America is at least 4–5 times higher compared to the amount of erupted products. Therefore, fluxes of volatiles estimated above should be at least 4–5 times higher if we take the flux of primary magmas into account.

The major uncertainty of the flux estimate comes, however, from the unknown amount of intruded magmas comprising the hidden magmatic flux, which cannot be assessed by studying volcanic products. Present-day volatile fluxes obtained by remote-sensing satellites or on-land-based techniques provide some clues to the magnitude of the total volatile fluxes (Hilton et al. 2002; Zimmer et al. 2004). Combined with data on concentrations of volatiles in parental magmas from this study, this allows us to estimate the total magmatic flux in Central America and the amount of intruded magmas. This calculation is however based on a major assumption: that present-day SO_2 fluxes are representative of long-term SO_2 fluxes determined from melt inclusions and volcanic fluxes estimated for the past $\sim$200,000 years.

The total SO_2 flux from volcanoes in Central America was estimated as 21.3×10^9 mol/year from COSPEC measurements (Hilton et al. 2002). Recalculated to mass units and normalized to 1 m of the arc length, this estimate gives S flux of 6.45×10^8 kg/m/Ma. This is $\sim$8 times more than our estimate of volcanic S flux (8.3×10^7 kg/m/Ma, Table 3) and suggests that volcanic rocks in Central America may account for $\sim$13% or less (since not all S will reach the atmosphere) of the total magmatic flux from the mantle to the lithosphere if the present-day SO_2 flux was constant over the past $\sim$200,000 years. By combining COSPEC SO_2 flux data (Hilton et al. 2002) with the average S content in parental magmas ($\sim$0.3 wt%, Table 3) and assuming complete degassing of magmas and that all the S reaches the atmosphere, we can estimate total magmatic flux in Central America as $\sim 2.2 \times 10^{11}$ kg/m/Ma. Volcanic products comprise $\sim$13% of this amount, $\sim$39% are

Table 3 Fluxes of volatiles in the Central American volcanic arc

Value	Unit	1: Guatemala	2: El Salvador	3: Western Nicaragua	4: Eastern Nicaragua	5: Northern Costa Rica	6: Central Costa Rica	7: average CA (volcanic)	8: average CA (total flux)	9: global average	10: CA/ global	11:subduction input	12: output/ input
Segment length	km	262	252	166	137	92	150	1,059					
Magma flux	kg/m/Ma	4.00E + 10	3.75E + 10	1.30E + 10	1.60E + 10	1.50E + 10	2.40E + 10	2.8E + 10	2.2E + 11	1.9E + 11	1.17		
Compositions of parental melts													
Ba/La (WR)		50	59	94	56	42	31						
La/Nb (WR)		3.1	3.1	2.1	1.9	3.5	2.8						
La/Y (WR)		0.7	0.36	0.26	0.28	0.6	1.1						
H_2O	Wt%	3.5	4.0	5.6	3.8	3.1	4*	4.0					
Cl	Wt%	0.09	0.09	0.06	0.06	0.10	0.08	0.08					
S	Wt%	0.31	0.31	0.24	0.23	0.34	0.29	0.29					
F	Wt%	0.04	0.02	0.02	0.02	0.03	0.05	0.03					
Estimate from volcanic flux													
H_2O flux	kg/m/Ma	1.41E + 09	1.48E + 09	7.33E + 08	6.10E + 08	4.71E + 08	9.60E + 08	1.1E + 09		9.1E + 09	0.12	3.51E + 10	0.03
S flux	kg/m/Ma	1.25E + 08	1.17E + 08	3.12E + 07	3.61E + 07	5.12E + 07	6.98E + 07	8.3E + 07		5.5E + 08	0.15		
Cl flux	kg/m/Ma	3.52E + 07	3.30E + 07	8.33E + 06	9.49E + 06	1.46E + 07	1.94E + 07	2.3E + 07		1.5E + 08	0.15	1.00E + 09	0.02
F flux	kg/m/Ma	1.50E + 07	8.75E + 06	2.49E + 06	3.19E + 06	5.01E + 06	1.31E + 07	8.9E + 06					
Estimate from SO_2 flux													
H_2O flux	kg/m/Ma								8.36E + 09	9.1E + 09	0.92	3.51E + 10	0.2
S flux	kg/m/Ma								6.45E + 08	5.5E + 08	1.18		
Cl flux	kg/m/Ma								1.80E + 08	1.5E + 08	1.19	1.00E + 09	0.2
F flux	kg/m/Ma								6.93E + 07				

Notes. Columns *1–6*: Data for single segments along the volcanic front. Magma fluxes correspond to volcanic fluxes after Carr et al. 1990, 2007). Mean ratios Ba/La, La/Nb and La/Y are calculated for primitive to moderately evolved ($SiO_2 < 54$ wt%) rocks from every segment (Centam data base; Carr et al. 2003). Concentrations of volatiles in parental melts are calculated from the mean trace element ratios (Figs. 10, 11, 12) except for H_2O concentrations in central Costa Rica (marked with '*'), which were assumed to be intermediate between Arenal and Irazú parental melts. Fluxes of volatiles were calculated from volcanic flux and concentrations of volatiles in parental melts; Column *7*: Length-normalized average estimate for volcanic flux, composition of parental melts and volatile fluxes for the Central American volcanic front; Column *8*: Total flux of magmas and volatiles in Central America estimated from COSPEC SO_2 flux data (Hilton et al. 2002) (underlined value). Fluxes of H_2O, Cl and F were calculated using volatile/S ratios in average parental melt from column *7*. Total magmatic flux was calculated from the COSPEC SO_2 flux and average sulfur content in parental melts; Column *9*: Average global arc-length-normalized fluxes of magma (recalculated from (Crisp 1984)) and volatiles (Wallace 2005) at volcanic arcs; Column *10*: Ratio of the length-normalized Central America fluxes to the global fluxes; Column *11*: Subduction-related input of volatiles to the Central American subduction zone. An estimate for H_2O includes only structurally bound H_2O in sediments and oceanic crust (1.8×10^{10} kg/m/Ma; Jarrard 2003) and H_2O in serpentinites (1.7×10^{10} kg/m/Ma, M. Ivandic, personal communication). Chlorine is stored in sediments and the oceanic crust (6.63×10^8 kg/m/Ma; Jarrard 2003) and serpentinites (3.4×10^8 kg/m/Ma assuming that serpentinites have sea-water-like $H_2O/Cl = 50$); Column *12*: Ratio of the length-normalized volatile flux outputs in Central America to the subduction input

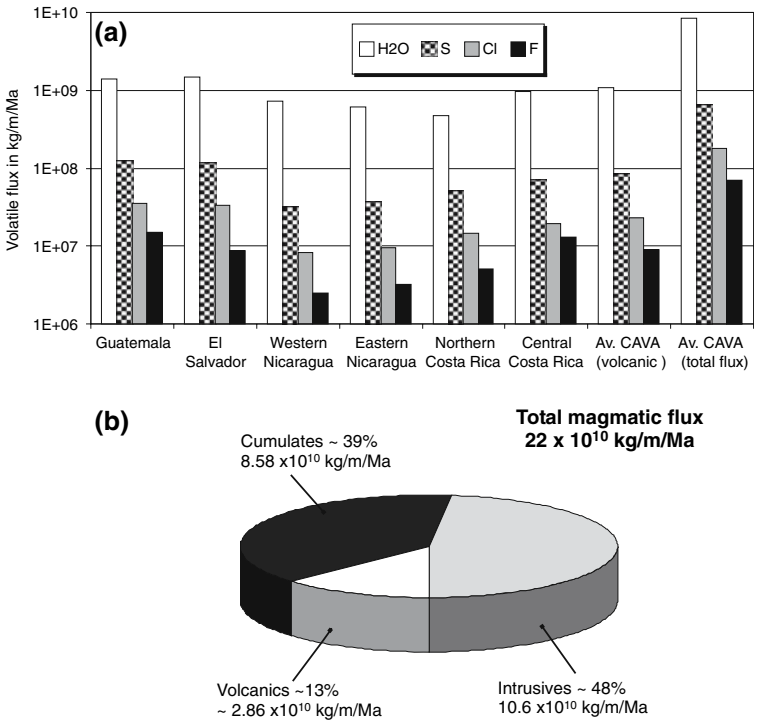

Fig. 13 Fluxes of magmas and volatile components in Central America. **a** Volcanic volatile fluxes estimated from inferred compositions of parental melts (this study) and published volcanic flux data (Carr et al. 1990, 2007), average length-normalized volcanic flux and total volatile flux estimated on the basis COSPEC SO_2 flux (Hilton et al. 2002); **b** mass-balance between volcanic output, amount of cumulates and amount of intrusives contributing to the total magmatic flux as estimated from the total COSPEC SO_2 flux (Hilton et al. 2002), volcanic fluxes (Carr et al. 1990, 2007) and compositions of parental melts (this study)

cumulates related to volcanism (assuming average 75% fractionation of parental melts), and the rest ~48% are intrusives solidified in the lithosphere (Fig. 13b). The amount of intrusives and total magmatic flux can certainly be larger as some S can be fixed in sulphide phases or released from degassing magmas at depth, thus remaining in the crust. Sulfur that never reaches the atmosphere, of course, cannot be accounted for by COSPEC measurements. Nevertheless, we note that the total magmatic flux for Central America ($\sim 2.2 \times 10^{11}$ kg/m/Ma) is surprisingly similar to the global average magma flux (1.9×10^{11} kg/m/Ma, based on the average global magma output in volcanic arcs of 2.5 km^3 (Crisp 1984 and assuming magma density 2.5 g/cm^3 and the total length of volcanic arcs world-wide of 33,000 km). The coincidence of both estimates is very remarkable as they were obtained in fully independent ways. Volatile fluxes in Central America are also quite similar to the global arc averages (Wallace 2005) (Table 3). These amounts represent significant mass fraction of volatiles initially stored in the subducting plate (Table 3). For example, average magmatic volatile fluxes account for ~20% of structurally bound water and chlorine in the Cocos Plate crust being subducted beneath Central America (Jarrard 2003).

Water flux versus magmatic productivity

Several authors have proposed that the amount of volatile elements (particularly H_2O) released from the subducting slab is larger beneath Nicaragua than Costa Rica (Ranero et al. 2003; Rüpke et al. 2004), which should result in a greater magmatic flux for Nicaragua. Our data demonstrate that mantle sources of magmas in Nicaragua are indeed more hydrated and generated magmas with somewhat higher H_2O content compared to Guatemala and Costa Rica (excluding Irazú Volcano). Calculated fluxes of H_2O are however similar along Central America or even lower in Nicaragua (Table 3, Fig. 13), reflecting the relatively low volcanic flux estimated for this region based solely on volcanic edifice volumes (Carr et al. 2007). Due to the many uncertainties in the present available data, it is difficult to judge if we have an adequate picture of magmatic fluxes along Central America, which limits our ability to determine accurate volatile fluxes. The total magmatic fluxes of volatiles in Nicaragua are likely to be under-estimated relative to other Central American arc segments, because (1) tephras not deposited on the volcanic edifices, which represent a significant proportion of the eruptives, were not included in the present volcanic flux estimates (A. Freundt and S. Kutterolf, personal communication) and (2) there may be a higher proportion of intruded to erupted magmas in Nicaragua compared to Costa Rica, consistent with evidence for a larger magmatic flux from the ~6 times greater fumarolic SO_2 flux from the Nicaraguan volcanoes (Frische et al. 2006) compared to those in Costa Rica (Zimmer et al. 2004). The amount of eroded volcanic rocks has also not yet been estimated, serving as another uncertainty in the volcanic fluxes.

Further studies aimed at quantifying magmatic fluxes along Central America clearly have potential to demonstrate correlation between the amount of volatiles delivered to the mantle and the magmatic flux. We note however that magmatic productivity (magmatic flux) and the amount of water delivered to the mantle do not have to be fully coupled in subduction zones. The amount of water in the mantle, which decreases the solidus of mantle peridotite, is certainly important but not the only factor enhancing melt production. Other important parameters affecting magmatic productivity are (1) mantle temperature, (2) source composition and (3) shape and volume of melting region. These factors are believed to govern magmatic productivity at ocean ridges and hot spots (Langmuir et al. 1992; McKenzie and Bickle 1988; Yaxley and Green 1998) and should be equally important in subduction zones (Carr et al. 1990; Kelley et al. 2006; Portnyagin et al. 2007). All parameters affecting the amount and composition of arc magmas should be taken into consideration in order to better understand the fluxes through the Central American subduction factory and the origin of island-arc magmatism in general.

Conclusions

We studied melt inclusions in olivine from volcanic rocks representing all major geochemical types of magmas from the Central American volcanic front. Inclusions were characterized for major and trace elements and volatiles (H_2O, S, Cl, S) by electron and ion microprobes. These results combined with literature data were used to estimate mean parental magma compositions and elucidate their origin in different segments of the Central American arc. The major conclusions from our study follow:

1. Geochemical systematics of primitive melts suggest that a large diversity of crustal (from subducting plate and overriding plates) and mantle (incoming plate and wedge) components are involved in the origin of geochemical zoning along the Central America volcanic arc. Large heterogeneity of melt inclusions from single rock samples implies that sources of magmas are highly heterogeneous on the small scale.
2. Two different trends of coupled Nb and LREE enrichment were recognized. High Nb/La (OIB-like) component contributes to the composition of some Nicaraguan magmas. In all other parts of the Central American Arc, the LREE- and Nb-rich component has relatively low Nb/La ($\sim$0.3) and most likely has a subduction-related origin through partial melting of subducting sediments and/or oceanic crust.
3. All parental melts are hydrous and contain $\sim$2–5 wt% H_2O, which correlates inversely with Ti, Y and Na and directly with Ba/La and B/La. These correlations are interpreted as indicating variable extents of melting of heterogeneous mantle sources fluxed by Ba- and B-rich water-bearing components at conditions close to the dry peridotite solidus. Cerro Negro Volcano in central Nicaragua with the highest Ba/La and the lowest $\delta^{18}O$ also had the largest amount of water estimated for the magma source of 1.7 wt% (with the exception of the anomalous Irazú Volcano). Central Nicaragua is also where the down-going plate was proposed to be particularly hydrated due to serpentinization at the outer rise.
4. Estimated abundances of volatile elements in parental magmas correlate with some trace element ratios (Ba/La, B/La, La/Nb, La/Y), which allow the extensive data base on whole rock compositions to be used to assess volatile concentrations in magmas along the entire volcanic arc. We suggest that the best proxy for H_2O in magmas of Central America (except central Costa Rica) is Ba/La but that B/La can also be used as a proxy for water. Chlorine and to lesser extent sulfur concentrations correlate with La/Nb ratio, whereas fluorine concentrations correlate with La/Y ratio.
5. We use concentrations of volatiles in parental melts and published data on volcanic fluxes to estimate fluxes of volatile elements for different segments of and for the entire Central American Arc. Flux of water was found to be similar throughout the Central American volcanic arc. Fluxes of other volatiles are somewhat lower in Nicaragua compared to Guatemala, El Salvador and Costa Rica. The estimates based on volcanic flux data can be informative of the relative magnitude of volatile fluxes along the volcanic front, if degree of crystallization and amount of intruded magmas are similar for all segments of the arc. The volcanic fluxes, however, define the lower limit of the true magmatic fluxes. The volatile fluxes estimated for Nicaragua could be underestimated, if there was a greater quantity of intrusion to extrusion in Nicaragua than in the rest of the arc.
6. Comparison of COSPEC data of total SO_2 flux from volcanoes with our estimates using melt inclusion volatile contents and the volcanic flux allows assessment of the total volatile and magmatic fluxes in Central America, which are $\sim$8 times higher compared with the volcanic flux and volatile fluxes using the volcanic flux. We estimate that volcanic products comprise $\sim$13% of the total magmatic flux, cumulates $\sim$39%, and intrusives solidified in the lithosphere the remaining $\sim$48%, which represent the 'hidden' fraction of the total magmatic flux. Total magmatic and volatile fluxes in Central America are similar to the independently estimated global averages.

Acknowledgments We would like to thank W. Strauch, G. Rocha, G. Alvarado, C. Ramirez, O. Mattius and G. Soto for field assistance, M. Thöner and S. Simakin for analytical assistance, and J. Phipps Morgan, L. Rüpke, T. Hansteen, M. Carr, K. Garofolo, A. Freundt, S. Kutterolf, H. Whermann and W. Perez for stimulating discussions on Central American arc magmatism. We are grateful to D. Hilton, L. Patino, P. Wallace, T. Plank and M. Carr for providing constructive and helpful comments on earlier versions of this manuscript. This work was funded by the Deutsche Forschungsgemeinschaft through Sonderforschungsbereich 574 "Volatiles and Fluids in Subduction Zones" to the University of Kiel and the Russian Foundation for Basic Research (grant 06-05-64873-a to M.P.). This is contribution number 76 to SFB 574.

References

Abers GA, Plank T, Hacker BR (2003) The wet Nicaraguan slab. Geophys Res Lett 30(2):1098–1101

Abratis M, Wörner G (2001) Ridge collision, slab-window formation, and the flux of Pacific asthenosphere into the Carribean realm. Geology 29(2):127–130

Aubouin J, Azema J, Carfantan J-C, Demant A, Rangin C, Tardy M, Tournon J (1982) The Middle-America Trench in the geologic framework of Central America. In: Initial reports of the ocean drilling program, vol 67, pp 747–755

Benjamin ER, Plank T, Wade JA, Kelley KA, Hauri EH, Alvarado GE (2007) High water contents in basaltic magmas from Irazú volcano, Costa Rica. J Volcanol Geotherm Res (in press)

Carr MJ, Feigenson MD, Bennett EA (1990) Incompatible element and isotopic evidence for tectonic control of source mixing and melt extraction along the Central American arc. Contrib Mineral Petrol 105:369–380

Carr MJ, Feigenson MD, Patino LC, Walker JA (2003) Volcanism and geochemistry in Central America: progress and problems. In: Eiler J (ed) Inside the subduction factory, vol.138, pp 153–174

Carr MJ, Saginor I, Alvarado G, Bolge LL, Lindsay FN, Turrin B, Feigenson MD, Swisher III CC (2007) Element Fluxes from the Volcanic Front of Nicaragua and Costa Rica. Geochem Geophys Geosyst 8:Q06001. doi:10.1029/2006GC001396

Carroll MR, Rutherford MJ (1988) Sulfur speciation in hydrous experimental glasses of varying oxidation states: results from measured wavelength shifts of sulfur X-ray. Am Mineral 73:845–849

Chaussidon M, Jambon A (1994) Boron content and isotopic composition of oceanic basalts: geochemical and cosmochemical implications. Earth Planet Sci Lett 121:277–291

Crisp JA (1984) Rates of magma emplacement and volcanic output. J Volcanol Geotherm Res 20:177–211

Danyushevsky L, McNeill AW, Sobolev AV (2002) Experimental and petrological studies of melt inclusions in phenocrysts from mantle-derived magmas: an overview of techniques, advantages and complications. Chem Geol 183:5–24

Duggen S, Portnyagin M, Baker J, Ulfbeck D, Hoernle K, Garbe-Schönberg D, Grassineau N (2007) Drastic shift in lava geochemistry in the volcanic-front to rear-arc region of the Southern Kamchatkan subduction zone: evidence for the transition from slab surface dehydration to sediment melting. Geochim Cosmochim Acta 71:452–480

Eiler JM, Carr MJ, Reagan M, Stolper E (2005) Oxygen isotope constraints on the sources of Central American arc lavas. Geochem Geophys Geosyst 6:Q07007. doi:07010.01029/02004GC000804

Feigenson MD, Carr MJ (1993) The source of Central American lavas: inferences from geochemical inverse modeling. Contrib Mineral Petrol 113(2):226–235

Feigenson MD, Carr MJ, Maharaj SV, Juliano S, Bolge LL (2004) Lead isotope composition of Central American volcanoes: Influence of the Galapagos plume. Geochem Geophys Geosyst 5:Q06001. doi:10.1029/2003GC000621

Frische M, Garofalo K, Hansteen TH, Borchers R (2006) Fluxes and origin of halogenated organic trace gases from Momotombo volcano (Nicaragua). Geochem Geophys Geosyst 7:Q05020. doi:10.1029/2005GC001162

Garrido CJ, Lopez Sanchez-Vizcaýno V, Gómez-Pugnaire MT, Trommsdorff V, Alard O, Bodinier J-L, Godard M (2005) Enrichment of HFSE in chlorite-harzburgite produced by high-pressure dehydration of antigorite-serpentinite: implications for subduction magmatism. Geochem Geophys Geosyst 6:Q01J15. doi:10.1029/2004GC000791

Goss AR, Kay SM (2006) Steep REE patterns and enriched Pb isotopes in southern Central American arc magmas: evidence for forearc subduction erosion?. Geochem Geophys Geosyst 7:Q05016. doi:10.1029/2005GC001163

Harris DM, Anderson AT (1984) Volatiles H_2O, CO_2 and Cl in a subduction related basalt. Contrib Mineral Petrol 87:120–128

Hilton DR, Fischer TP, Marty B (2002) Noble gases and volatile recycling in subduction zones. In: Porcelli D, Ballentine C, Weiler R (eds) Noble gases in geochemistry and cosmochemistry, reviews in mineralogy and geochemistry, vol 47. Mineralogical Society of America, Washington, DC, pp 319–370

Hoernle K, Werner R, Phipps Morgan J, Garbe-Schonberg D, Bryce J, Mrazek J (2000) Existence of complex spatial zonation in the Galápagos plume. Geology 28(5):435–438

Hofmann AW (1988) Chemical differentiation of the Earth: the relationship between mantle, continental crust and oceanic crust. Earth Planet Sci Lett 90:297–314

Hofmann AW (2003) Sampling mantle heterogeneity through oceanic basalts: isotopes and trace elements. In: Treatise on geochemistry, vol 2. Elsevier, Amsterdam, pp 61–101

Ionov DA, Hofmann AW (1995) Nb-Ta-Rich mantle amphiboles and micas—implications for subduction-related metasomatic trace-element fractionations. Earth Planet Sci Lett 131(3–4):341–356

Jarosewich EJ, Nelen JA, Norberg JA (1980) Reference samples for electron microprobe analysis. Geostand Newslett 4:43–47

Jarrard RD (2003) Subduction fluxes of water, carbon dioxide, chlorine, and potassium. Geochem Geophys Geosyst 4(5):8905 doi:10.1029/2002GC000392

Katz RF, Spiegelman M, Lagmuir CH (2003) A new parameterization of hydrous mantle melting. Geochem Geophys Geosyst 4(9):1073. doi:1010.1029/2002GC000433

Kelley K, Plank T, Grove TL, Stolper EM, Newman S, Hauri E (2006) Mantle melting as a function of water content beneath back-arc basins. J Geophys Res 111:B09208. doi:10.1029/2005JB003732

Langmuir CH, Klein EM, Plank T (1992) Petrological systematics of mid-ocean ridge basalts: constraints on melt generation beneath ocean ridges. In: Phipps Morgan J, Blackman DK, Sinton JM (eds) Mantle flow and melt generation at mid-ocean ridges, vol 71. AGU, Washington, DC, pp 183–280

Leeman WP, Carr MJ, Morris JD (1994) Boron geochemistry of the Central American Volcanic Arc: constraints on the genesis of subduction-related magmas. Geochim Cosmochim Acta 58(1):149–168

Lundstrom CC, Hoernle K, Gill J (2003) U-series disequilibria in volcanic rocks from the Canary Islands: plume versus lithospheric melting. Geochim Cosmochim Acta 67(21):4153–4177

McKenzie D, Bickle MJ (1988) The volume and composition of melt generated by extension of the lithosphere. J Petrol 29:625–679

Morris JD, Leeman WP, Tera F (1990) The subducted component in island arc lavas: constraints from Be isotopes and B-Be systematics. Nature 344:31–36

Patino LC, Carr MJ, Feigenson MD (2000) Local and regional variations in Central American arc lavas controlled by variations in subducted sediment input. Contrib Mineral Petrol 138:265–283

Plank T, Langmuir CH (1998) The chemical composition of subducting sediment and its consequences for the crust and mantle. Chem Geol 143:325–394

Portnyagin MV, Simakin SG, Sobolev AV (2002) Fluorine in primitive magmas of the Troodos Ophiolite Complex, Cyprus: analytical methods and main results. Geochem Int 40(7):625–632

Portnyagin MV, Hoernle K, Plechov PY, Mironov NL, Khubunaya SA (2007) Constraints on mantle melting and composition and nature of slab components in volcanic arcs from volatiles (H_2O, S, Cl, F) and trace elements in melt inclusions from the Kamchatka Arc. Earth Planet Sci Lett 255(1–2):53–59

Protti M, Gündel F, McNally K (1995) Correlation between the age of the subducting Cocos plate and the geometry of the Wadati-Benioff zone under Nicaragua and Costa Rica. In: Mann P (ed) Geologic and tectonic development of the Caribbean plate boundary in southern Central America, vol 295, pp 309–326

Ranero C, Phipps Morgan J, McIntosh K, Reichert C (2003) Bending-related faulting and mantle serpentinization at the Middle America trench. Nature 425:367–373

Roggensack K (2001a) Sizing up crystals and their melt inclusions: a new approach to crystallization studies. Earth Planet Sci Lett 187(1–2):221–237

Roggensack K (2001b) Unraveling the 1974 eruption of Fuego volcano (Guatemala) with small crystals and their young melt inclusions. Geology 29(10):911–914

Roggensack K, Hervig RL, McKnight SB, Williams SN (1997) Explosive basalic volcanism from Cerro Negro volcano: influence of volatiles on eruptive style. Science 277(9):1639–1642

Rüpke L, Phipps Morgan J, Hort M, Connolly JAD (2002) Are the regional variations in Central American arc lavas due to differing basaltic versus peridotitic slab sources of fluids? Geology 30(11):1035–1038

Rüpke LH, Phipps Morgan J, Hort M, Connolly JAD (2004) Serpentine and the subduction zone water cycle. Earth Planet Sci Lett 223(1–2):17–34

Salters VJM, Stracke A (2004) Composition of the depleted mantle. Geochem Geophys Geosyst 5(5):Q05004. doi:05010.01029/02003GC000597

Sisson TW, Layne GD (1993) H_2O in basalt and basaltic andesite glass inclusions from 4 subduction-related volcanoes. Earth Planet Sci Lett 117(3–4):619–635

Sobolev AV, Chaussidon M (1996) H_2O concentrations in primary melts from island arcs and mid-ocean ridges: implications for H_2O storage and recycling in the mantle. Earth Planet Sci Lett 137:45–55

Sobolev AV, Hofmann AW, Kuzmin DV, Yaxley GM, Arndt NT, Chung S-L, Danyushevsky LV, Elliott T, Frey FA, Garcia MO, Gurenko AA, Kamenetsky VS, Kerr AC, Krivolutskaya NA, Matvienkov VV, Nikogosian IK, Rocholl A, Sigurdsson IA, Sushchevskaya NM, Teklay M (2007) The amount of recycled crust in sources of mantle-derived melts. Science 316:412–417

Stolper E, Newman S (1994) The role of water in the petrogenesis of Mariana Trough magmas. Earth Planet Sci Lett 121(3–4):293–325

Sun S-S, McDonough WF (1989) Chemical and isotopic systematics of oceanic basalts: implications for mantle composition and processes. In: Saunders AD, Norry MJ (eds) Magmatism in the ocean basins, vol 42. Geological Society Special Publication, London, pp 313–345

Syracuse EM, Abers GA (2006) Global compilation of variations in slab depth beneath arc volcanoes and implications. Geochem Geophys Geosyst 7:Q05017. doi:10.1029/2005GC001045

Wade JA, Plank T, Melson WG, Soto GJ, Hauri EH (2006) The volatile content of magmas from Arenal volcano, Costa Rica. J Volcanol Geotherm Res 157(1–3):94–120

Walker JA, Carr MJ, Feigenson MD, Kalamarides RI (1990) The petrogenetic significance of interstratified high- and low-Ti basalts in Central Nicaragua. J Petrol 31(5):1141–1164

Walker JA, Roggensack K, Patino LC, Cameron BI, Matias O (2003) The water and trace element contents of melt inclusions across an active subduction zone. Contrib Mineral Petrol 146:62–77

Wallace PJ (2005) Volatiles in subduction zone magmas: concentrations and fluxes based on melt inclusion and volcanic gas data. J Volcanol Geotherm Res 140(1–3):217–240

Werner R, Hoernle K, van den Bogaard P, Ranero C, von Huene R, Korich D (1999) Drowned 14-m.y.-old Galápagos archipelago off the coast of Costa Rica: implications for tectonic and evolutionary models. Geology 27(6):499–502

Werner R, Hoernle K, Barkckhausen U, Hauff F (2003) Geodynamic evolution of the Galápagos hot spot system (Central East Pacific) over the past 20 m.y.: Constraints from morphology, geochemistry, and magnetic anomalies. Geochem Geophys Geosyst 4(12):1108. doi:10.1029/2003GC000576

Yaxley GM, Green DH (1998) Reactions between eclogite and peridotite: mantle refertilisation by subduction of oceanic crust. Scweiz Miner Petrogr Mitt 78:243–255

Zimmer MM, Fischer TP, Hilton DR, Alvarado GE, Sharp ZD, Walker JA (2004) Nitrogen systematics and gas fluxes of subduction zones: Insights from Costa Rica arc volatiles. Geochem. Geophys. Geosyst. 5:Q05J11 doi:10.1029/2003GC000651